The International Journal of Advanced Manufacturing Technology
https://doi.org/10.1007/s00170-024-14610-8

CRITICAL REVIEW

Process enhancement and performance evaluation of single-shot drilling of CFRP/aluminum stacks: a review

Joy Mathavan Jebaratnam[1] · Muhammad Hafiz Hassan[2,3]

Received: 20 June 2024 / Accepted: 2 October 2024

Abstract
Drilling is an essential process in the construction of aircraft panels made from composite/metal stack materials, and it has a considerable impact on the performance of the aircraft during flight and its overall lifespan. Among CFRP/Al/Ti, CFRP/Ti, and CFRP/Al stacks, CFRP/Al panels are widely used in the aviation industry. This paper examines in detail the developments made in the drilling of stacks made of carbon fiber reinforced polymer (CFRP) and aluminum (Al), with the goal of determining how different machining parameters affect the quality of the holes. The primary requirements for aircraft components are to attain a low level of hole surface roughness, minimize burr heights, reduce the diameter difference in stack-up, and minimize delamination. The subject matter encompasses a wide range of tool shapes, materials, drilling parameters, and innovative methods of cooling and coating, all with the goal of reducing hole damage and improving quality. In addition, the paper examines several forms of hole damage and presents modern methodologies for their quantification. This review study aims to develop a reliable standard for achieving accuracy, optimal productivity, and reducing harm in the drilling procedure of CFRP/Al stacks in aerospace applications. Future works on analysis of bond strength, hardness, and coefficient of friction of coated drill bits and application of nano fluid-based coolants may further enhance the drilling quality.

Keywords CFRP/Al stack · Damage tolerance · Surface analysis · Machining

Abbreviations

AL	Aluminum alloy
AlTiSiN-G	Aluminum titanium silicon nitride coating
BUE	Build-up edge
BUL	Build-up layer
CARALL	Carbon reinforced aluminum laminate
CFRP	Carbon fiber reinforced plastic
CFRP/Al	Carbon fiber reinforced polymer/aluminum
CVD	Chemical vapor deposition
C7	Nano-crystalline AlTiN grains embedded in an amorphous matrix of silicon nitride (Si_3N_4)
DF	Delamination factor
DLC	Diamond like carbon
FMC	Fiber metal composite
GFRP	Glass fiber reinforced plastic
GLARE	Glass reinforced aluminum laminate
HSS	High speed steel
HSS-Co	High speed steel with cobalt binder
HP-LF MQL	High pressure low frequency minimum quantity lubrication
LN_2	Liquid nitrogen
LP-HF MQL	Low pressure high frequency minimum quantity lubrication
MD CFRP	Multi directional carbon fiber reinforced plastic
MoS_2	Molybdenum di sulfide
MQL	Minimum quantity lubrication
PC	Percentage of contribution
PCBN	Polycrystalline cubic boron nitride
PCD	Polycrystalline diamond
PCR	Partial correlation regression

✉ Muhammad Hafiz Hassan
mhafizhassan@usm.my

1 Department of Engineering Technology, Faculty of Technology, University of Jaffna, Kilinochchi Premises, Ariviyal Nagar, Kilinochchi 44000, Sri Lanka

2 School of Mechanical Engineering, Engineering Campus, Universiti Sains Malaysia, Nibong Tebal, 14300 Pulau Pinang, Malaysia

3 Advanced Machining Lab, Gandtrack Asia Sdn Bhd, 75350 Ayer Keroh, Melaka, Malaysia

Published online: 30 October 2024

PMC	Polymer matrix composite
PVD	Physical vapor deposition
ta-C	Tetrahedral amorphous carbon
ta-C:Cr	Chromium dopant added tetrahedral amorphous carbon
Ti	Titanium alloy
TiN	Titanium nitride coating
TiAlCr	Titanium aluminum chromium
TiAlN	Titanium aluminum nitride
TiSi	Titanium silica
TiSiN	Titanium silica nitride
WC	Tungsten carbide

1 Introduction

When manufacturing multi-material parts for aerospace structures, metals like aluminum or titanium stacked up with composite panels are frequently used these days [1]. Among CFRP/Al/Ti, CFRP/Ti, and CFRP/Al stacks, CFRP/Al panels are widely used in the aviation industry due to the salient features of carbon fiber reinforced plastic (CFRP) and aluminum. Composites have high stiffness-to-weight ratio, high strength-to-weight ratio, good fatigue strength [2], good damage tolerance, excellent specific strength, good corrosion resistance, good dimensional, and chemical stability [3]. Metals consist of isotropic structure, high impact strength, high bearing strength, and are easily repairable. Specifically, aluminum have superior qualities like high fatigue strength, high thermal conductivity, lightweight, and excellent workability [4]. The combined advantages of metal and composite are the reason behind metal-composite stack material being used in aircraft industry. In general, CFRP is extensively used in structural applications as it is stiffer than titanium and more resilient than steel while maintaining the strength [5]. By using composite materials into airplane constructions, fuel efficiency, pollution control, and weight carrying capability have been improved [5–9]. Fiber metal laminates (FML) can be made using thin sheets of metallic alloy and composite material that are adhered together with adhesives like epoxy due to their strong bonding abilities and easiness of manufacturing [10–12]. Epoxy resins are widely used in fiber metal composites (FMC) since they possess outstanding heat and chemical resistance, excellent electrical insulating qualities, low density, and outstanding elastic modulus.

In aircraft constructions, single-shot drilling is used to produce holes of various sizes and depths [13]. Single shot drilling varies from the conventional drilling in the following aspects. In single-shot drilling, a single drill bit is used to drill through all layers of stacked materials like CFRP/Al stack in one continuous operation. It is faster and more efficient because it completes the drilling in a single pass, reducing the need for tool changes or multiple drilling operations. But conventional drilling typically involves drilling one layer/type of material at a time or using multiple operations for different materials (e.g., drilling CFRP first, then drilling aluminum). It takes longer time because it involves separate processes or steps for different materials. For stacked materials, it may require flipping or repositioning the workpiece or changing tools. Therefore, drilling of fiber-reinforced composite materials compared to drilling of metallic materials, in single-shot drilling, introduces special obstacles as its manufacturing activity varies in different aspects [14–17]. Not only the product being anisotropic and inhomogeneous [18–20], but the action also depends on the orientation of the fiber and its properties [21]. Inappropriate selection of drilling parameters including speed and feed or configuration of drill bits may also cause various types of damages like delamination, fiber-matrix debonding, pull up or push down fibers, splintering, geometrical defects, and thermal alterations [22, 23]. Tool wear is also an undesirable occurrence in the drilling phase when drilling a composite since this has an impact on geometry and quality of the workpiece's drilled surfaces, especially in the hole diameter [24].

Therefore, the primary goal of this study is to present an in-depth analysis of single-shot drilling of carbon fiber reinforced composites/aluminum (CFRP/Al) stacks by concentrating on the crucial problems in the industry and provide possible solutions. Although few review studies have addressed the drilling of carbon fiber reinforced composites/titanium (CFRP/Ti) stacks, none of them concerns specifically on manufacturing defects and process improvement for the drilling of CFRP/Al stacks. First, the key features of material usage in aircraft industry will be discussed in terms of FMC, and composite/metal stacks. The key findings of experiments conducted by the industry and academicians over the past years on single-shot stack up drilling process advancements and their impact on hole quality will then be outlined. Then, the performance measurements of the manufacturing defects in terms of drilling forces, delamination, dimensional accuracy, hole surface roughness, and burr formation will be addressed. By emphasizing relevant findings from the literature, this research strives to bring forth the techniques of drilling CFRP/Al stacks bearing in mind the damage suppression. It also aims to assist researchers and industry in selecting the most effective ways for high-performance drilling.

2 Commercial aircraft assembly

Aerospace industries have become more interested in fiber metal laminates due to its better mechanical and physical qualities including excellent impact and fire resistance, high strength-to-weight ratio, and outstanding corrosion and erosion resistance [9, 25–27]. Despite the fact that they are typically manufactured in a close-to-net shape for necessary precision in assembly, more complex components require secondary machining processes. To this end, the most important machining for applying rivets and screws during part assembly is drilling. Various literature studies mentioned that three hundred thousand to three million holes may be present in commercial aircraft and majority of them deal with holes of diameters of 4–8 mm [2, 11, 28–37]. This indicates that drilling is an important procedure used in aircraft manufacturing and it has a direct effect on the flight characteristics and lifespan of the aircraft [38]. Drilling of composite/metal stacks like CFRP/Ti, CFRP/Al, and CFRP/Al/Ti with minimum hole surface roughness, stack up diameter difference between panels, and burr height that abides close tolerance for aircraft components is a difficult task [39, 40]. Their inherent differences in machining properties present the biggest problem when drilling a stack of metal and composite materials. Poor hole quality due to roundness, surface roughness, chipping, etc., produced by improper machine setup typically results in rejection. Therefore, to prevent defects in the drilled hole, it is crucial to have a fundamental knowledge of the interaction between the cutting-edge of the drill and the material being drilled [41, 42]. For example, cutting conditions between metals and composites in single-shot drilling differ in terms of the chip generation during drilling [43]. While superior hole surface roughness in composites requires continuous chip formation [44], discontinuous chip creation is better machining characteristic for metals [20, 26]. However, since the composite part is formed from layers that produce dust-type chips, it is very difficult to make continuous chips for composite part [37]. Therefore, drilling ductile aluminum and highly abrasive carbon fiber require the right cutting tool and process parameters selection.

The best method for reducing processing time and positioning error is single-shot drilling of stacked metal/composite panels [39, 40]. However, an appropriate drill bit for both metal and composite materials is needed for single-shot drilling of the CFRP/Al considering the drilling mechanism of the tool. The same material may be cut differently by different cutting edges, and the same cutting edge may simultaneously cut metal and CFRP. Thus, throughout the combined machining process, the force acting on various parts of the cutting edge is completely different and will fluctuate constantly. In particular, when the stack up comprises of a metal portion, the unique geometric design of drills such as straight flute drills or spur drills which is suitable for composite drilling is not suited for stack up material drilling [38]. The majority of earlier studies used the standard twist drills when drilling metal/composite stacks [25, 37, 45–48]. In contemplation of achieving better hole quality, particularly at the composite portion, most researchers selected tungsten carbide (WC) as cutting tool material because of its high wear resistance and strength compared to high-speed steel (HSS) tools or high-speed steel with cobalt (HSS-Co) [49, 50].

2.1 Fiber metal composite laminates

Fiber reinforced composite and thin layers of alloy are combined into a single laminate using the autoclave procedure to create FMC laminates as an alternative material to fiber-reinforced composites or metals [2]. The primary goal of FMC is to address the shortcomings of metal's corrosion resistance and fatigue strength as well as poor impact strength, bearing strength, and repairability issues of composite materials [51]. FMC have been divided into many groups, such as those based on aluminum, titanium, and magnesium, depending on the type of metal utilized. The FMC made of aluminum can be divided further into three groups depending on the bonded fiber reinforced composite such as carbon-reinforced aluminum laminate (CARALL) [52, 53], glass reinforced aluminum laminate (GLARE) [2, 54–56], and aramid reinforced aluminum laminate (ARALL) [52, 57]. These FMC have advantages including high tolerance against impact damage and fatigue crack growth while being used in structural applications such as aircraft, compared to the conventional laminates which consists only of sheet fiber reinforced composite ply or monolithic metal (mostly aluminum or titanium) [51]. Boeing and Airbus, the main aircraft manufacturers, are switching from conventional aerospace alloys to FMC in their new aircraft models. The analysis of the use of titanium, aluminum, and composite materials in various commercial aircrafts is shown in Fig. 1. It reveals a rise in composite and a decline in aluminum in the aviation industry. The data of Fig. 1 are derived from references [31, 58].

Since about 1930, aluminum alloys presented the most commonly utilized material for the structural elements of airplanes [58] such as fuselage, wings, and supporting structures of commercial aircraft as well as military cargo and transport planes. Although polymer matrix composites (PMC) have been broadly utilized in high-performance military planes and some applications in contemporary commercial planes, the continued respect for aluminum alloys has long been a result of a sum of factors such as familiar performance characteristics, known fabrication cost, substantial body of design knowledge, and extensive production methods and facilities [58]. Due to its light weight, aluminum can easily replace other metals and withstand pressure loads on wings that have increased as a result of the development of larger aircraft [59]. Though there are various grades of aluminum alloys, aerospace sector mostly prefers the grades come from the 2000 and 7000 series [60].

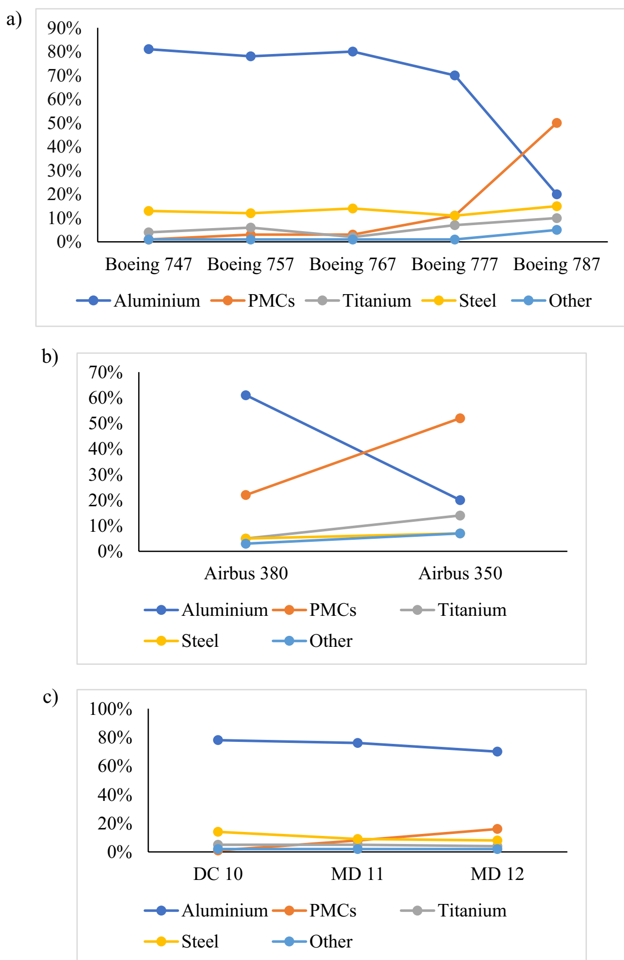

Fig. 1 The percentage usage of materials in (**a**) Boeing, (**b**) Airbus, and (**c**) McDonnell Douglas aircrafts

Alloys from the 2000 series have better tolerance for damage and exhibit good resistance to the development of fatigue cracks. As a result, they are frequently utilized in aircraft's lower wings and fuselage skins, where a crucial design factor is fracture toughness [61]. Al2024-T3 is the most widely utilized 2000 series alloy in fuselage construction [62]. The primary design factor for the upper wing skins where the 7000 series is usually utilized is strength [61]. The most well-known alloy from the 7000 series for usage in aircraft applications is Al7075-T6 [63]. Copper makes up 3–4% of the primary alloying constituents in the Al 2000 series, whereas zinc makes up 6–7% of the alloying constituents in the Al 7000 series. The friction stirs welding process, which was developed in 1991, can be used to combine these two series of aluminum, which are typically not weldable by conventional methods. Since riveting is the acknowledged traditional method of attaching fuselage and wing structures, the weldability of the high strength 2000 and 7000 series of aluminum alloys used to make fuselage and wing parts is extremely low [64].

It has become more common these days to create stack materials with CFRP, titanium, and or aluminum since metals can only be partially replaced at the moment [65]. CFRP/Al and CFRP/Ti stack are the most common structures among them [66]. In general, this is true for systems like structures used in aerospace that are vulnerable to dangerous mechanical loads [67]. These materials require high-quality hole drilling and joining. Different structural characteristics (such as unique elastic components, thermal expansion coefficient) usually make it difficult to achieve the necessary tolerances. Severe tool wear, roundness deviation, heat-induced damage, and metal burr formation are the most common issues when cutting these incompatible materials [47].

3 Process improvement in drilling of stacked material

It is highly recommended and necessary to conduct a machinability analysis of CFRP/Ti, CFRP/Al, or CFRP/Al/Ti structures for aerospace applications, mostly due to its enormous potential [68, 69]. Conventional drilling is a frequently used process in manufacturing airplanes [70]. Tool temperature, tool wear, changes in dynamic cutting forces, hole damage, and chip disposal are some major issues with multi-material stack drilling [25, 47, 71]. These problems account for approximately 60% of all part rejections [11, 55, 59, 72–75]. This section covers the recent researches conducted on customization of drill geometry, optimization of drilling parameters, application of coating, and implementation of cooling environment, and it shows that each of these actions plays an important role on process improvement of stack up drilling. Each of the following sub-sections discuss these advancements in detail.

3.1 Customization of drill geometry

The point angle, helix angle, primary clearance angle, and chisel edge angle are the four main tool geometry variables that have an impact on the cutting mechanism. The detailed tool geometry is shown in Fig. 2 [76]. Khan mentioned that drill's cutting edge is tougher and less likely to chip when the helix angle is lower, but it also produces higher cutting forces and temperatures [77]. Primary clearance is essential to avoid the workpiece from being rubbed by the drill's flank. A large clearance angle will extend the tool's life since it reduces friction, but at the expense of tool's strength, since it decreases as the primary clearance angle increases [77]. The point angle is the first point of contact that cuts the fibers and matrix while drilling [78], and it is more efficient to cut the CFRP by a sharper point angle (110°) as the cutting area is small which in turn will reduce the delamination

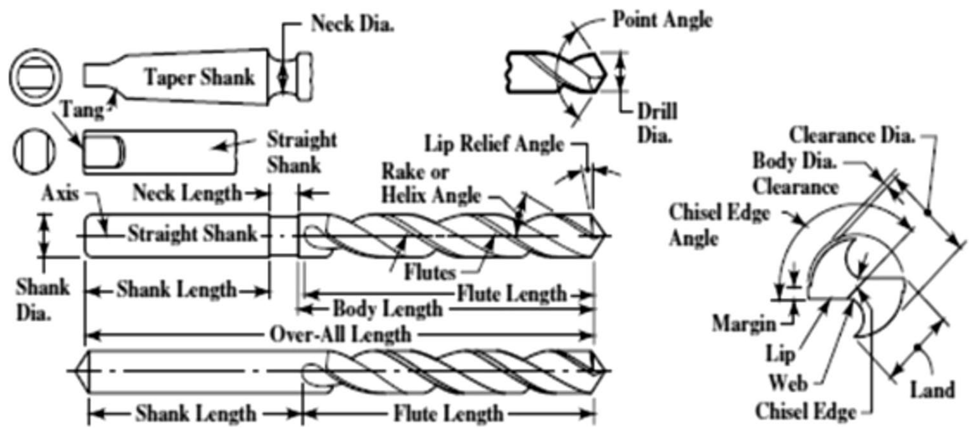

Fig. 2 Detailed tool geometry of a twist drill [76]

damage [79]. Regarding the chisel edge angle, the longer cutting lips created at a lower chisel edge resulted in a more effective cutting operation [80].

According to Hassan et al., the tool geometry has a big impact on generated thrust force. They mentioned that, when performing single shot drilling in CFRP/Al stack, the drilling process generates the minimum thrust force in CFRP panel when the point angle is 110°, primary clearance angle is 6°, chisel edge angle is 30°, the feed rate is 0.05 mm/rev, and spindle speed is 1500 rev/min. Increasing the helix angle yields a reduction in the thrust force for the Al7075-T6 panel, while it had no influence on the CFRP panel. With regard to the Al7075-T6 panel, the optimal results are achieved when the point angle is 130°, helix angle is 30°, chisel edge angle is 30°, the feed rate is 0.05 mm/rev, and the spindle speed is 1500 rev/min [80]. They further mentioned that, for CFRP panel, the point angle and chisel edge angle appear to be important factors in determining the peak thrust force value in addition to the feed rate, since a lower point angle and chisel edge angle corresponds to a lower peak thrust force [80].

In another research by Hassan et al., the CFRP panel showed the least amount of thrust force (81.16 N) when maximum chisel edge angle (PC 8.87%) and maximum primary clearance angle (PC 58.78%) were combined. The Al7075-T6 panel also showed the lowest thrust force (180.67 N) when maximum chisel edge angle (PC 12.19%) and maximum primary clearance angle (PC 52.34%) were combined (Fig. 3(c)) [81]. They revealed that, for drilling CFRP/Al7075-T6 stacks in a single shot drilling, the combined set of 45° chisel edge angle (Fig. 3(a, c)), 130° point angle (Fig. 3(a)), and 7° primary clearance angle (Fig. 3(d)) drill geometry resulted in the lowest possible thrust force and the smoothest possible hole surface [81]. According to Wei et al., a rise in point angle results in an increase in thrust force and a decrease in torque, whereas an increase in chisel edge and helix angles produces a drop in thrust force and torque [82]. Additionally, it has been claimed that drill bits with narrow chisel edges can help provide less thrust force, enhance heat dissipation area, and reduce thermal expansion of composite and thereby minimize damage caused by delamination [83, 84]. Because of less workpiece material being prone to plastic deformation, there will be shorter burr formation near the hole's exit and more material being cut as opposed to being extruded as the result of the chisel's short edge [65]. To prevent material degradation, which might in return affect the degree of delamination, the drill bits should be designed to produce the least amount of heat [85]. Table 1 summarizes the researches on the thrust forces obtained for single shot drilling of CFRP/Al stacked up materials using various drill bit geometries and drilling parameters. It can be seen that, with the rise in feed rate, the thrust force in both Al and CFRP panels increases. Besides that, the thrust force in aluminum panel is greater than that in the CFRP panel.

When it comes to the hole size, Hassan et al. mentioned that the primary reason for the bigger hole sizes in Al7075-T6 than CFRP is mostly attributed to the greater helix angle of 30°. A greater helix angle enhances the lifting force, facilitating effective and consistent removal of chips during the machining process. Conversely, the bigger hole sizes in CFRP than Al7075-T6 are due to the occurrence of continuous chip development. When chips are formed continuously, they can get stuck and not be removed easily. This can cause the hole in the CFRP material to become larger [80].

When analyzing the formation of burr height, a twist drill with a large point angle produces smaller burrs by altering the direction of chip flow. According to Hassan et al., this alteration facilitates rapid movement of the cutting edge, minimizing the risk of work hardening [81]. It was possible to suppress the minimum burr height by 89.1% by raising the point angle from 110° to 130° as shown in Fig. 4. It was also stated that while using a tool with a point angle of 130°, the burr height varied from 133.62 to 211.45 µm, and when using a tool with a point angle of 110°, it varied from 1036.25 to 2066.85 µm. According to their observations, drills with 110°-point angle produced transitory and

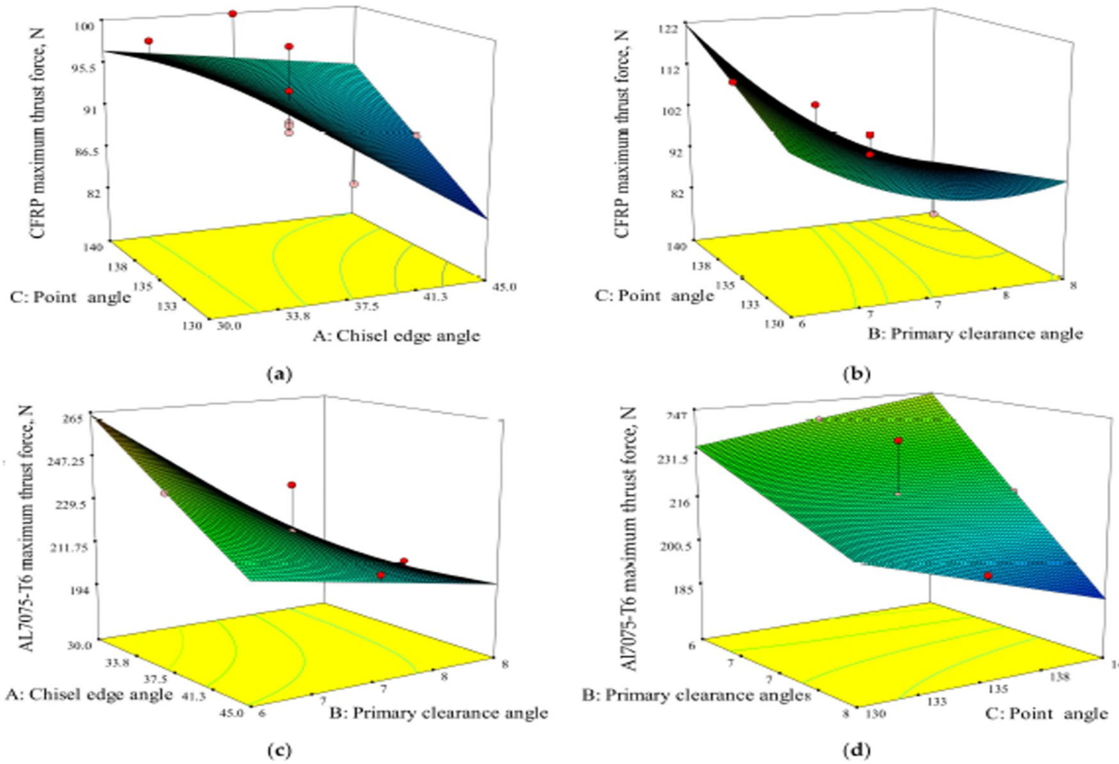

Fig. 3 3D response surface for maximum thrust force for CFRP: (**a**) chisel edge angle and point angle, (**b**) primary clearance angle and point angle. 3D response surface for maximum thrust force for Al7075-T6: **c** chisel edge angle and primary clearance angle, (**d**) point angle and primary clearance angle [81]

Table 1 Maximum thrust force obtained for single shot drilling of CFRP/Al stacked up materials while changing the drilling parameters

Tool diameter (mm)	Type of tool	Parameters				Maximum thrust force		
		Feed rate (mm/rev)	Spindle speed (rev/min)	Point angle (°)	Helix angle (°)	CFRP (N)	Al (N)	Author
6.35	Twist drill with double cone type drill	1. 0.05 2. 0.10 3. 0.15	2020	90 132	-	1. 80 2. 100 3. 122	1. 180 2. 330 3. 486	[37]
6.00	Uncoated solid carbide twist drill	1. 0.05 2. 0.10 3. 0.15	2750	136	-	1. 108 2. 142 3. 180	1. 285 2. 486 3. 658	[86]
8.00	Uncoated twist drill	0.1	1050	118	-	100	250	[87]
6.00	1. Uncoated twist drill 2. Diamond coated 3. TiAlCrN coated 4. AlTiSiN-G coated	0.04	3000	124	30	1. 40 2. 100 3. 60 4. 70	1. 120 2. 180 3. 140 4. 140	[88]
6.35	Twist drill (tungsten carbide)	0.05	2020	90 132	-	50	300	[44]
6.80	Solid carbide twist drill	0.06	3500	-	-	300	450	[89]
6.80	Solid carbide twist drill coated with TiCN	0.06	3050	-	-	250	300	[90]
9.53	Diamond coated drill bit with double tip point angles	1. 0.02 2. 0.08	2000	130/60	30	1. 100 2. 175	1. 200 2. 325	[20]

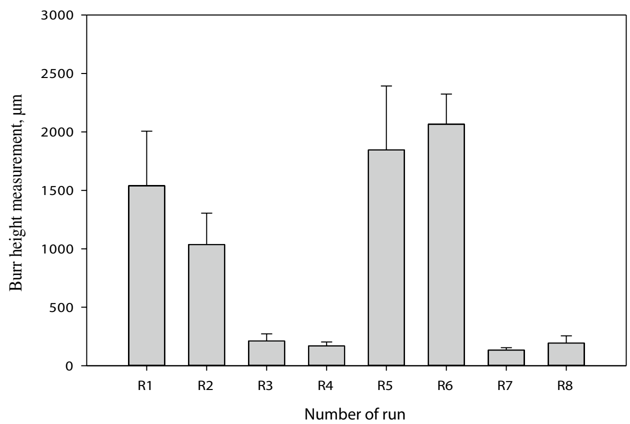

Fig. 4 Maximum burr formation value for different combination of tool geometry (R1, R2, R5, and R6 are with 110° point angle; R3, R4, R7, and R8 are with 130° point angle [38])

crown burrs, whereas drills with 130°-point angle created uniform burr type [81]. In addition, they noticed that raising the primary clearance angle from 6° to 8° led to a modest rise in burr height of 7.13%, and raising the helix angle and chisel edge angle increased the burr height by 43.41% and 25.92%, respectively. This is owing to the fact that there was not enough room for chips to evacuate, which increased the likelihood of chips obstructing the drill flutes. Congested chips constantly rub against the hole wall cause heat to produce in the drill and the area around the drill flute which makes the workpiece more ductile and eventually leads to high burr height. In a different experiment by Hassan et al., lower burr height was discovered at 130°-point angle, 6° primary clearance angle, and 45° chisel edge angle while higher burr height was discovered at 135°-point angle, 7° primary clearance angle, and 30° chisel edge angle [38]. The drill cap must also present at the hole's exit so that a consistent and minimal burr height may be achieved.

When considering the surface roughness, the average roughness of the CFRP panel during the drilling of Ti/CFRP/Al stack panels is significantly influenced by the orientation of the individual ply fibers and the sharpness of the tool corner, according to Kuo et al. The friction between the workpiece and the drill bit would increase when the drill bit's outer edge wore down and it was observed that, as the tool became more worn, the CFRP hole surface roughness also increased [91]. This friction caused problems such as the separation of layers, empty spaces, fibers sticking out, cracks in the material, and resin sticking to the surface that was drilled. Studies show that when a low point angle and primary clearance angle are combined with a high chisel edge angle, the CFRP panel achieves the smoothest hole surface roughness of 0.4649 μm. Additionally, when a higher chisel edge angle is combined with a lower point angle and primary clearance angle, the Al7076-T6 material has the least surface roughness (0.2423 μm) [81]. Furthermore, Xu et al. discovered that drilling at a lower point angle produced a fine dust chip of composite material [92]. The better the hole surface roughness that may be attained, the finer the dust chip that the particular bit shape can create [93]. According to Hassan et al., the lowest hole surface roughness is achieved with a drill bit geometry of 45° chisel edge angle and 6° primary clearance angle. If the primary clearance angle is set too high (8°), the tool's cutting edge weakens and chipping becomes more noticeable [81].

Special geometry drill bits were also occupied to carry out stack drilling by some researchers. The drilling performance of a high-strength CFRP composite panels using a regular twist drill (Fig. 5(a)) and a customized "dagger drill" (Fig. 5(d)) was discussed by few researchers [94–96]. However, because of the insufficient chip evacuation capability of the narrow helix angle, the "dagger drill" is not advised for aluminum/titanium panels, but the smaller helix angle and point angle of the dagger drill provided superior surface finish such as less delamination damage and less burr defect than the twist drill design. The single-shot drilling of CFRP/Al stack combinations was also found to be improper with double cone geometry drill (Fig. 5(c)), because, even when performing at minimum parameter combination, the system catastrophically failed after only four holes [39]. This was brought on by the drill flutes' extreme chip packing and adhesion, which prevented the removal of swarf from the hole. Various drills experimentally tried for stack up drilling are shown in Fig. 5. Zhang et al. compared a twist drill (Fig. 5(a)) and a special geometry candle stick drill (Fig. 5(e)) with varying feed and speed. They mentioned that small diameter tolerance (less than 5 μm), burr height (50 to 80 μm), burr root thickness (around 5 μm), and hole wall roughness (for CFRP within 2 μm, and for Al 7075-T7 within 1 μm) are because of the tool geometry rather than the cutting parameters [65]. This is because the special geometry candle stick drill bit's two-stage point configuration offered an enhanced "self-centering" ability, resulted in improved tool positioning and superior hole precision [65, 97]. It was also stated by some other researchers that, regardless of the drill type utilized, the chip would damage the drilled hole diameter and surface roughness of CFRP while evacuation [45, 98, 99].

While many studies on stack-up drilling have been conducted in recent years, most of the work conducted using direct comparisons of specialized and ordinary tools with one or more characteristics of drilling responses. They merely describe the possible relation between tool geometry, tool material, and other functions like cutting parameters. A solid fit between these parameters and perfect tool shape is yet to be find. Additional study is required to explore and establish the ideal combination of tool attributes for optimal performance in stack-up drilling.

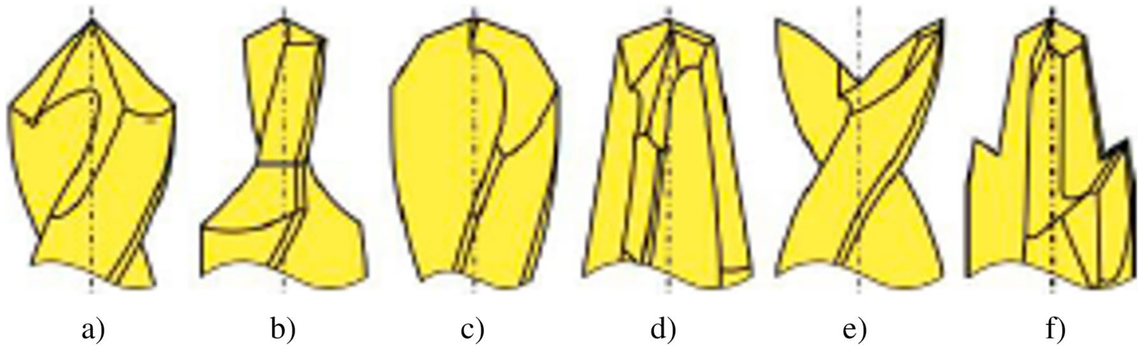

Fig. 5 Advanced drilling tools: **a** twist drill with a small point angle; **b** step drill; **c** double point angle twist drill; **d** dagger drill (also known as one-shot drill); **e** fishtail drill; **f** brad and spur drill (also known as candlestick drill) with a dagger type center [100]

3.2 Optimizing drilling parameters

The impact of optimizing the drilling parameters on process improvement can be analyzed from various grounds such as chip size and form, thrust force and torque, and hole quality. This section explains about the influence of drilling parameters on these factors. When considering the chips, the most important component for the quality of a drilling operation is the form and size of the chip. Researches showed that material, feed rate, drill type, cutting fluid, drill speed, and coatings are the key factors impacting chip size [101, 102]. If the chips are well broken, the drilling operation will be smooth. CFRP chips are fragmented into tiny dust particles during drilling CFRP/Al stacks due to its high brittle nature, layered structure, and anisotropic property. As the drill passes to the aluminum panel from the CFRP panel, it creates a continuous aluminum chip. Generally, ductile materials tend to undergo a continuous chip production instead of fracturing when subjected to drilling. Nevertheless, a reduced feed rate and elevated cutting speed can impede chip breakability, resulting in the formation of continuous chips [37]. Increasing the depth of cut can potentially improve chip breakability, which is evaluated by the number of chips in 100 g of chips. However, the determination of the ideal depth of cut is dependent upon both the feed rate and the drill diameter. The impact of the drill diameter and feed rate on chip breakability is substantial, since it leads to an enlargement of the chip's cross-sectional area, hence enhancing its stiffness [37]. Chip breaking was simple and effective for feed rates of 0.1 mm/rev and higher and for drill diameters of 6 mm and above. Additionally, it was noted that while drilling CFRP/Al using 6-mm and 4-mm drills, the increase in torque and thrust force was significantly less than when using an 8-mm drill. This is explained by the chip's sharply rising cross-sectional area and the longer chisel edge length that comes with higher diameters [37]. Nevertheless, the impact of spindle speed on chip breakability and therefore on torque and thrust force was less pronounced in comparison to the feed rate. Zitoune et al. [45] indicated that, while drilling CFRP panel in CFRP/Al stack, the size and shape of the chip are unaffected by the choice of cutting parameters; nevertheless, when drilling aluminum panel, the feed rate has a prominent effect on the size and shape of the chip, as shown in Fig. 6, regardless of the drill or coating employed. Additionally, they said that no change in chip size or form was seen while spindle speed was increased within the range 1050–2750 rev/min. Usually polymer composite chips are continuous at low feed rates, and as the feed rate grew, the chips turn into dust [103]. But when the feed rate is low, and the spindle speed is high, aluminum chips produce continuously [89].

Hassan et al. also mentioned that the size and shape of chips generated while drilling Al7075-T6 panel of a stack up panel with a fixed-diameter twist drill are significantly influenced spindle speed. When operating at a lower spindle speed of 1500 rev/min, the low shearing rate allows for easy winding of chips, resulting in the development of long, continuous chips [80]. However, as the speed raised to 2600 rev/min, the higher shearing speed causes the chips to become stiffer and more resistant to winding, breaking them into smaller spiral pieces. Lower feed rates result in smaller shearing areas, facilitating smoother chip evacuation since the chips created at 0.05 mm/rev have more uniform size and shape [80]. Kim et al. mentioned that when the feed rate is small and the cutting speed is large, the production of aluminum chips is continuous [103]. They also mentioned that continuous chip is formed when drilling a composite panel using small feed rate, and it changes to dust-like chips as the feed rate is raised [103]. A continuous, high-temperature aluminum chip would pass through the CFRP panel hole when aluminum is layered at the bottom of the composite. Long chips tend to impede their efficient movement through the flutes, which, in turn, leads to increased torque, elevated temperatures, and an elevated risk of drill breakage [98]. However, when operating at a speed of 2600 rev/min with a feed rate of 0.05 mm/rev, chip development reaches an optimal state. This results in the creation of compact, closely wound chips as well as serrated and fragmented

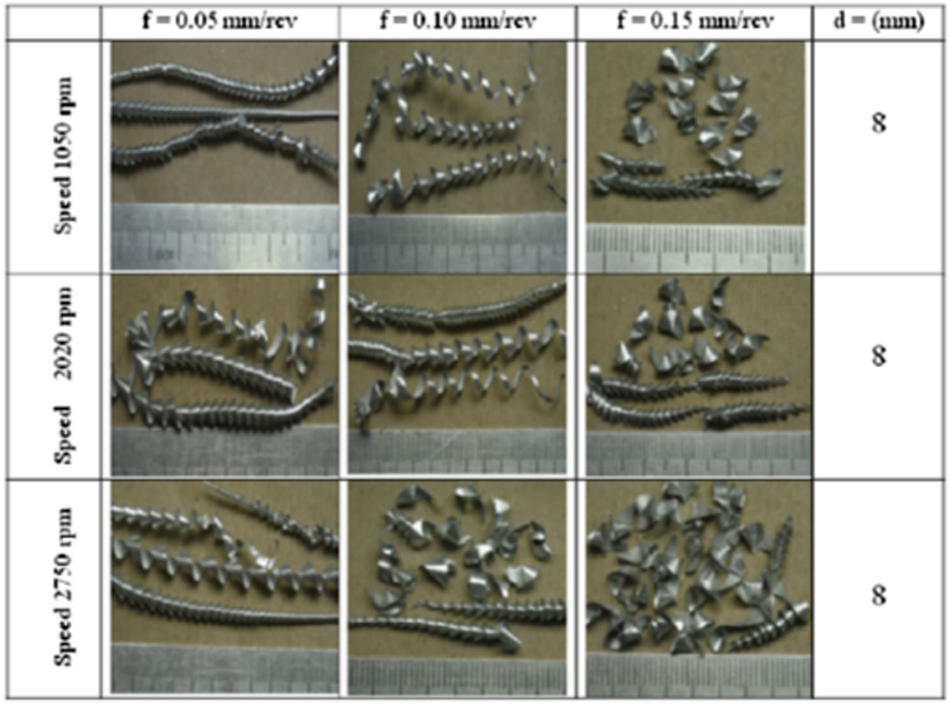

Fig. 6 Chip characteristics of CFRP/Al composites: speed versus feed on chip size [37]

chips. Spiral cone-shaped chips facilitate their easy ejection and, consequently, aid in efficient chip evacuation during the drilling process. The preference generally lies with shorter chips and tightly wound helical chips, as they contribute to a superior surface finish on the workpiece [104].

When considering the impact of drilling parameters on process improvement based on thrust force and torque, Chen stated that the impact of cutting speed on torque and thrust force while drilling multidirectional (MD) and unidirectional (UD) CFRP is negligible [17]. However, Liu et al. emphasized the considerable importance of the feed rate, as demonstrated by Figs. 7 and 8 [105]. Soo et al. agreed with this, affirming that changes in cutting speed did not have any influence on thrust force. However, elevating the feed rate to 0.30 mm/rev from 0.15 mm/rev caused the torque and thrust forces in the CFRP and aluminum layers of the stack to significantly rise—with maximum increases of 100% and 60%, respectively [39]. Ramulu et al. and Liu et al. mentioned that the optimum situation for drilling composite panels is with high speed and low feed rate [25, 105], while Ramulu et al. and Kurt et al. stated that high feed rate and high speed are optimum for aluminum alloys [25, 106]. Kuo et al. concluded that small spindle speed and large feed rates are harmful for hole drilling in composites since high damages were caused by these conditions [91]. However, Nouari et al. noted that using a WC tool to drill AA2024 is appropriate when the feed rate and the cutting speed is low [101]. Zitoune et al. when drilling CFRP/Al stacks observed that the torque and thrust force during aluminum drilling at 0.05 mm/rev is twice as high compared to CFRP drilling. However, at 0.1 mm/rev and 0.15 mm/rev, this difference increases to approximately three times higher. This disparity can be attributed to the diminished effective clearance angles of the drill, causing friction within the CFRP/Al stack and the intensified impact of the fibers [37]. They further mentioned that at larger spindle speeds, the thrust force of CFRP decreases because of the elevated temperature of cutting edges, which, in turn, decreases the cutting resistance of epoxy. Rawat and Attia also noted that reducing cutting speeds within the feed rate range of 0.02 to 0.08 mm/rev resulted in a substantial rise in the thrust force [107]. Conversely, when drilling aluminum, a faster spindle speed increases the thrust force as shown in Fig. 7 [37]. According to Won et al., at low feed rates, the thrust force attributable to the chisel edge makes up 40% of the total thrust force; and at high feed rates, this amount rises to 60% [108]. Additionally, as the number of holes drilled increased in the Al portion, a gradually declining trend in thrust force was noted by Soo et al. This could be related to a rise in temperature and consequent softening of the material as the trials went on [39].

The features that affect the hole surface finish significantly are material to be drilled, machining parameters, and the drill type [107]. When considering the impact of drilling parameters on process improvement, spindle speed and feed rate are two machining parameters that affect processing quality and precision, with feed rate having a bigger impact than spindle speed [109]. Some researches advised drilling of stack up materials using correct machining parameters consist of high feed rate and high speed to reduce continuous chip formation [25, 47]. Hassan et al.

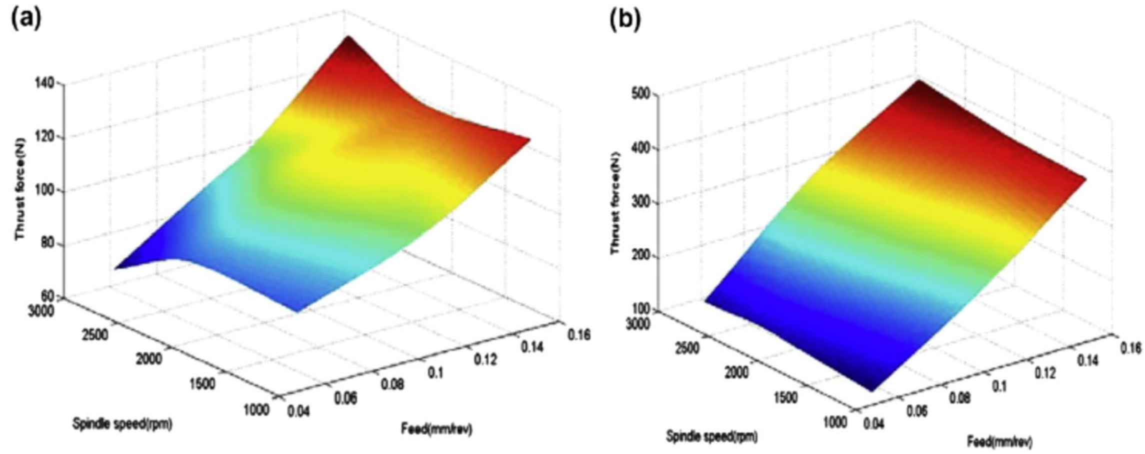

Fig. 7 Effect of spindle speed and feed rate on thrust force for U8 mm drill: **a** CFRP material and (**b**) aluminum material [37]

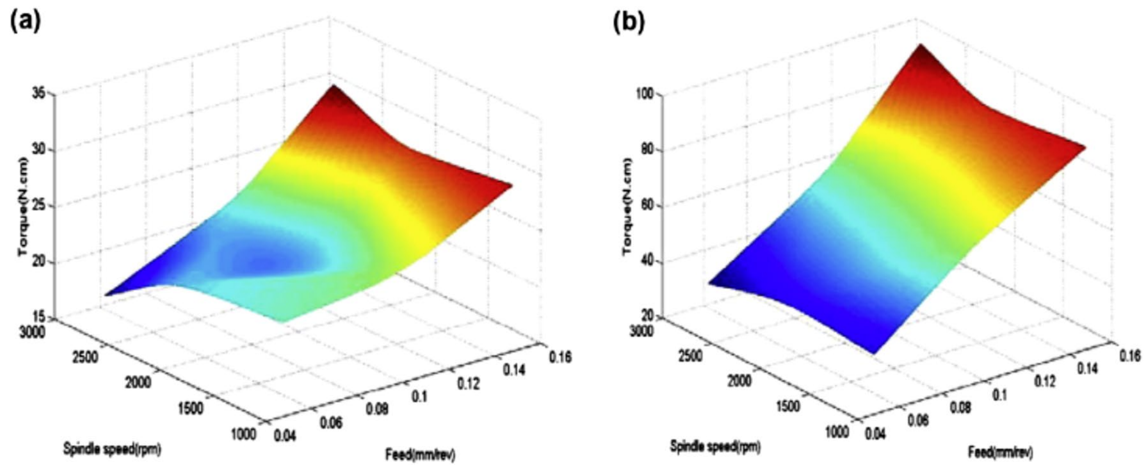

Fig. 8 Effect of speed and feed on torque for U8 mm drill: **a** CFRP material and (**b**) aluminum material [37]

mentioned that the optimum parameters for machining stacked materials are a feed rate of 0.05 mm/rev and a spindle speed of 2600 rev/min [80]. They further mentioned that the selection is driven by the benefits of using a lower feed rate, which allows for a gradual material removal at a shallower depth, ultimately resulting in an improved surface finish. However, in the aerospace industry, specific customer requirements dictate a fixed feed rate of 0.1 mm/rev and speed of 2600 rev/min, primarily to prioritize efficiency and time considerations [80]. When considering the surface roughness, it increased on both CFRP and Al panels after increasing the feed rate from 0.02 to 0.08 mm/rev while using diamond-coated cemented carbide tool [90]. When employing nc-CrAlN/a-Si_3N_4-coated tool [45] and uncoated tool [37], it is found that the roughness increases with increasing feed rate from 0.05 to 0.15 mm/rev on both CFRP and Al panel for different speeds. When the feed rate is low at 0.05 mm/rev, continuous chips are created, and the machining quality is improved with the least amount of surface roughness. The chips become broken at larger feed rates (between 0.1 and 0.15 mm/rev), which increases the surface roughness and thrust force irrespective of drill type [37, 45]. Contradictorily, Brinksmeier and Janssen mentioned that, creation of continuous aluminum chip can increase the surface roughness at low feed rate and spindle speed at both CFRP hole wall and the hole entry as the revolution of drill body with lengthy, hot, and sharp metal chips can hamper the surface finish and spoil the composite hole wall during evacuation [48]. According to Zitoune et al., surface roughness values of approximately 2–4 µm have been observed for CFRP at small feed rates of 0.05 mm/rev, independent of drill diameters and spindle speed. Additionally, when the feed rate rises, so does the surface roughness [37]. Contradictorily, Angelone et al. mentioned that internal roughness is affected by spindle speed as compared to feed rate [110]. According to Benezech et al., machining parameters have greater impact on CFRP's surface roughness than they do on aluminum as illustrated in Fig. 9 [111] and it is due to the anisotropy of CFRP material [37].

Experiments conducted on CFRP/Al panel to test the influence of feed rate and speed on drilled hole diameter by Wang et al. show that a greater spindle speed can result in improved CFRP and aluminum panel's diameter tolerance when the speed is raised from 1000 to 3000 rev/min with diamond-coated cemented carbide tools. The maximum stack-up diameter error at 1000 rev/min, 2000 rev/min, and 3000 rev/min were 50 µm, 35 µm, and 11 µm, respectively [90]. Soo et al. agreed with it saying that the diameter difference between first and last hole reduced when increasing speed to 120 m/min from 60 m/min while drilling CFRP/AA7010-T7451 with CVD diamond-coated WC drill [39], but Kim et al. mentioned that the diameter increases with increasing speed and metal holes are consistently have larger hole diameters than composite holes [47]. According to Wang et al., when feed rate rose to 0.08 mm/rev from 0.02 mm/rev, the diameters of aluminum, CFRP exit, and CFRP entrance showed a rising pattern. This was explained by instability of the drilling state and vibration of the drilling process [90]. Contradictorily, Soo et al. mentioned that the diameter was decreasing with increasing feed rate from 0.15 to 0.3 mm/rev [39].

When a hole is measured for roundness, it may be determined how closely its circular cross-section resembles a real circle, whereas cylindricity quantifies the cylinder's overall deviation from the true circle [46]. According to Kuo et al., when considering hole cylindricity, higher feed rate results in lower hole cylindricity in a way that, at a feed rate of 0.05 mm/rev, hole cylindricity was around 150 µm; however, at a feed rate of 0.08 mm/rev, it dropped to 100 µm [91]. Soo et al. also agreed with it saying that higher feed rate results in lower hole cylindricity at elevated speeds of 120 m/min, but at lower speeds of 60 m/min with increasing feed rate, the hole cylindricity also increases [39]. They also found that higher speed results in lower hole cylindricity and lower discrepancy between first and last hole when increasing the speed to 120 m/min from 60 m/min. As can be seen from Fig. 10, at low feed rates of 0.05 mm/rev, the circularity of the hole in CFRP was around 6 µm; as feed rates increase to 0.15 mm/rev, the circularity error rises to 25 µm [37]. Moreover, the out of roundness for CFRP was higher than that of AA7010-T7451 as the drill pierced the top layer of CFRP, potentially due to tool runout generating initial chisel edge sliding or radial deflection [97].

Soo et al. found that while using a larger feed rate of 0.30 mm/rev, delamination factor increased up to 23% because of the stronger thrust forces produced [39]. On one hand, serious damages were found even in the initial hole in the form of uncut or frayed fibers, and on the other hand, the delamination was barely influenced by the effects of cutting speed, tool wear, and the quantity of holes drilled. Meanwhile, Graham T Smith mentioned that continuous chips in aluminum will affect the composite's hole quality at the top of the hole with low feed rates by causing peel-up delamination [112]. According to Zitoune et al., when the amount of airborne dust increases, the vacuum system's effectiveness decreases

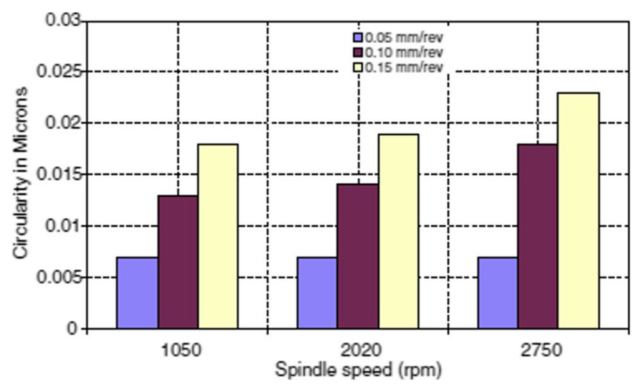

Fig. 10 Effect of spindle speed and feed on circularity of CFRP [37]

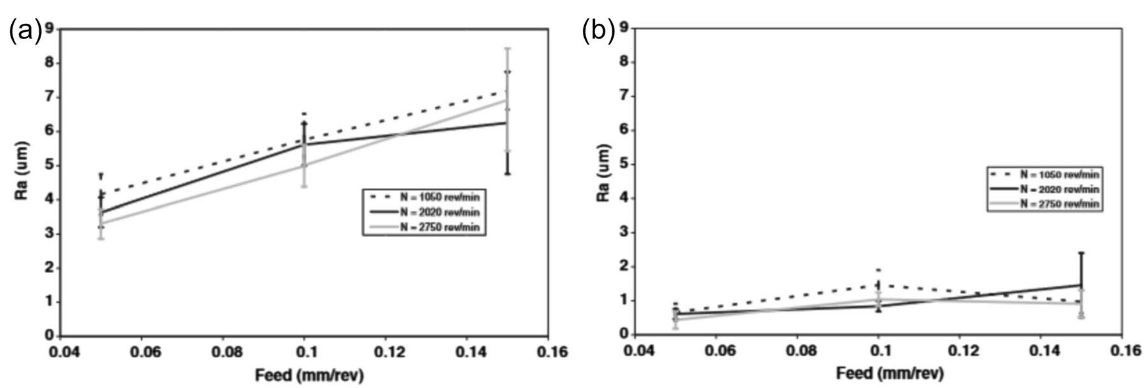

Fig. 9 Hole surface roughness versus feed rate at various spindle speeds for (**a**) CFRP and (**b**) Al panels during single-shot drilling of CFRP/Al stack up panel [37]

Table 2 Influence of speed and feed on various machining outputs

Speed	Feed	Result	Researcher
Increase	Decrease	Al discontinuous chip	[37]
Increase	Decrease	Al continuous chip	[89, 103]
Increase	Increase	Al continuous chip	[25, 47]
Decrease	Decrease	Al continuous chip	[98]
	Decrease	CFRP Continuous chip	[103]
	Increase	CFRP Dust chip	[103]
	Increase	Roughness increase	[37, 45]
Decrease	Decrease	Roughness increase	[98, 101, 102]
Increase	Decrease	Roughness decrease	[117, 118]
	Increase	Burr height increase	[65, 113]
	Increase	Burr height decrease	[114]
Increase	Not much change	Burr height decrease	[116]
Increase		Entry delamination increased	[119, 120]
Increase		Entry delamination decreased	[121]
Increase		Exit delamination increased	[23, 119, 120, 122]
Increase		Exit delamination decreased	[121, 123, 124]
Increase		No/Slight effect on entry delamination	[34, 125]
Increase		No/Slight effect on exit delamination	[34, 126]
	Increase	Entry delamination increased	[23, 34, 125–127]
	Increase	Exit delamination increased	[121, 125, 128, 129]
Increase	Decrease	Delamination decreased	[117, 130]
Increase	Decrease	Optimum for CFRP panel	[25, 91, 105]
Increase	Increase	Optimum for Al panel	[25, 106]
Decrease	Decrease	Optimum for Al panel	[101]
	Increase	Optimum for stack-up panel	[81]
Decrease	Increase	Thrust force increase	[9, 14, 37, 107, 113]

with the presence of continuous chips [20]. Therefore, using a higher feed rate of 0.1 mm/rev is the most optimal parameter to compensate for both CFRP and aluminum hole quality [81].

According to Zhang et al., with larger feed rate, the burr height tends to increase. The cutting zone's temperature and strain rate vary based on the spindle speed and feed rate, which affects the materials' ductility and strength [65]. As a result, the root thickness and burr height increases. Small feed rate of 0.05 mm/rev is necessary to ensure that the minimum thrust force is provided to minimize the burr growth [113]. Soo et al. also said that the exit burr width and height grew with growth in feed rates from 0.15 to 0.3 mm/rev, and were at least twice as large as those at the entrance's interlayer point, which was between 15.3 and 32.5 µm [39]. In contrast, Rivero et al. obtained the minimum burr height when increasing the feed rate when drilling a Ti/CFRP/Al stack [114]. Kelly and Cotterell also say that raising the feed rate would result in a smaller exit burr [115]. It was found that burrs at the exit and entrance were less at a larger feed rate of 0.08 mm/rev, perhaps because low thrust forces caused less plastic deformation of the workpiece [91]. Contradictory results were also obtained that the maximum burr height was unaffected by altering the feed rate to 0.1 mm/rev from 0.05 mm/rev, although an increase in spindle speed reduced the burr height by 32.39% [116].

Table 2 shows the experiments performed by various authors regarding the impact of tool feed and cutting speed on several output parameters such as surface roughness, delamination, and burr height. This table shows that different authors got varying outputs while changing the speed or feed. Therefore, it leads to the conclusion that the outputs are not solely dependent on feed and/or speed. Based on this conclusion, Table 3 is constructed. Table 3 not only consists of the cutting parameters but also contains cutting environment, tool geometry, tool material, and workpiece material details as well. This table further elaborates the outputs related to hole finish and tool wear behavior, chip formation and evacuation, thrust force, and torque details.

3.3 Usage of polycrystalline diamond

Cutting tools with high toughness, high hardness, high wear resistance, high thermal conductivity, and improved chemical insensibility are typically favored to obtain the best drill bit criterion to drill stack-up materials [136, 137].

To effectively cut the workpiece, the cutting tool's hardness should be higher than that of the workpiece. The resistance to indenter penetration is known as hardness [138]. Temperatures during drilling CFRP/Al stack can reach up to 200 °C [139]. To sustain such high temperatures, drills with hot hardness are essential. Hot hardness is the capacity to sustain high hardness at high temperatures. To be able to handle shock loads, vibration-induced chipping and cracking, misalignment, runouts, and other drilling process flaws, the tools should possess high toughness. Toughness is described as the material's capacity to absorb energy before breaking. Materials used to make drill bits move in the opposite direction in terms of hardness and toughness as can be seen in Fig. 11. For example, PCD, the hardest material, has the least toughness since its sharp deformation occurs at 600 °C, whereas high-speed steel (HSS), which has the highest toughness, deforms at a temperature of 700 °C [122, 140]. Therefore, increasing drill bit toughness while maintaining hardness is a key trend in the industry. In single-shot drilling applications, several tool materials, such as WC, high-speed steel (HSS), and super hard materials like polycrystalline cubic boron nitride (PCBN) and poly crystalline diamond (PCD), have been studied so far.

PCD is the hardest material used for manufacturing cutting tools and it is an artificially created incredibly hard material made by encasing diamond particles in a metal matrix. Vickers hardness (HV) of 6000 for PCD is significantly higher than that of WC (HV range of 1600–2200). Because of their high abrasion resistance [94, 95], high-speed drilling capability [141], and high thermal conductivity [142, 143], PCD tools have better cutting efficiency when drilling standard composites [144]. The PCD coating can also provide outstanding wear resistance due to its low friction properties when used for stack-up drilling and effectively mitigate the extreme adhesion of the chips found in metal part drilling [144]. Tools with primary diamond content and PCD tools are frequently used for stack-up drilling purpose [91, 145–148]. Because of manufacturing challenges and high costs, PCD tools, in contrast to WC, have a relatively small market share [29, 149].

It was discovered by Garrick et al. that, after 200 successfully completed holes, the 86-series PCD veined drill had to have its cutting edge re-sharpened since wear appeared on the cutting edge. The helical PCD drill outperformed conventional WC drills in terms of overall performance, but it was more susceptible to changes in feed rate when delamination was considered [67, 150]. In actuality, it was demonstrated that the core drill was stronger than the traditional twist drill. A novel core drill design showed a 26% reduction in delamination during composite drilling because of the drop in thrust force, drilling temperature, and surface clogging. This is one of the notable benefits of core drilling with a solid PCD drill [151]. Additionally, the veined PCD drills upgraded with K-land design outperformed traditional geometric PCD drills in terms of hole performance and tool life. A PCD drill, however, can readily fracture when machining either aluminum or titanium panel with high-speed particularly when layered with composites since PCD is inherently fragile [150]. As a result, it is advised that PCD drills be used with a comparatively lower range of cutting parameters than WC drills. Besides drill geometry and drilling parameters, drilling environment also have an important part in hole quality, which will be discussed next.

3.4 Cooling applications

To improve the effectiveness of stack up drilling experiments, several cooling techniques such as cryogenic cooling, flood cooling, and minimum quantity lubrication (MQL) can be used. A schematic diagram of cooling set up is shown in Fig. 12. Low-temperature liquefied gas is used in cryogenic cooling as cutting fluid. Liquid nitrogen (LN_2) or liquefied carbon dioxide (LCO_2) are typically employed due to their low cost and wide range of applications [152]. MQL is a green manufacturing process that can replace traditional dry and wet cutting with flow rates between 10 and 100 ml/h [153]. According to Iskander et al. and Meshreki et al., a combination of low oil flow rate and high air pressure is advantageous for the MQL drilling to achieve improved machining quality [154, 155], due to oil microparticles' superior penetration in the tool-chip contact [43]. However, it is advised against using flood cooling because the oil could enter the polymer matrix and change its mechanical properties [156].

3.4.1 Impact of cooling on thrust force

When a workpiece is being machined, the cutting tool slides against the workpiece as it removes material, and this creates the cutting force. Thrust force is one of the main scales used to assess the machinability of various composite/metal stacks and at high feed rates the power consumption also. It also affects the quality of holes and tool wear during drilling operations [14, 88, 132, 147]. Janakiraman et al. conducted cooling-related experiments on CFRP/GFRP/Al stacks and observed that, in cryogenic and MQL conditions, maximum and minimum thrust forces were produced, respectively [158]. When liquid nitrogen (LN_2) was used in cryogenic conditions, it increased the thrust force by 68.6%. This was due to the rise in Young's modulus and tensile strength of the CFRP-GFRP composite layers brought about by the abrupt drop in temperature [158]. At cryogenic temperatures, the epoxy matrix stiffens, enhancing the fibers' stiffness, which causes shear breakage of fibers instead of bending and tearing [72, 159]. The hardness of the aluminum alloy (Al 1100)

Table 3 Summary of testing of drill bit geometry and drilling parameters used for drilling a CFRP/Aluminum stack up

Drilling parameter	Tool & Environment	Workpiece	Findings	Author
(a) Spindle speed: 1050 rev/min to 2750 rev/min (b) Feed rate: 0.05 mm/rev to 0.15 mm/rev	(a) Size: 4 mm, 6 mm, and 8 mm (b) Dry condition	(a) CFRP/AL 2024 (b) Total thickness: 7.2 mm	Thrust force & torque, Surface roughness, Hole circularity, Delamination Chip behavior & BUE	[37]
(a) Spindle speed: 3050 rev/min (b) Feed rate: 0.06 mm/rev	(a) Uncoated WC, CVD diamond coating, hard metal C7 layer coated (b) Spray mist and wet cutting	(a) Ti-6Al-4 V/CFRP/AL7050 T7451 (b) Total thickness: ~ 10 mm	Effect of coating type Hole size & Burr height Hole surface roughness Micro hardness	[46]
(a) Spindle speed: 1050 rev/min to 2750 rev/min (b) Feed rates: 0.05 mm/rev to 0.15 mm/rev	(a) Uncoated carbide and nc-CrAlN/a-Si_3N_4 coating (b) Dry cutting	(a) CFRP/AL 2024 (b) Total thickness: 7.25 mm	Shape and size of the chips Surface roughness	[45]
(a) Spindle speed: 6000 rev/min (b) Feed rates: 0.02 mm/rev to 0.08 mm/rev	(a) Point angle: 120° to 150° (b) Rake angle: 0°to 40° (c) Dry cutting	(a) CFRP T800M21/Al 2024 (b) Total thickness: 10 mm	Axial rake angle Included angle	[111]
(a) Spindle speed: 3000 rev/min (b) Feed rate: 0.04 mm/rev	(a) Uncoated carbide, diamond, TiAlCrN and AlTiSiN-G coating (b) Dry cutting	(a) CFRPT800/AL7010 (b) Total thickness: 21 mm	Thrust force, BUE, Surface roughness, Holes diameter error, Delamination, Tool wear	[88]
(a) Spindle speed: 2000 rev/min (b) Feed rate: 0.03 mm/rev to 0.25 mm/rev	(a) Uncoated carbide and AlTiN coating under dry cutting (b) Point angle: 120° to 133.4° (c) Helix angle: 25° to 30° (d)Chisel edge angle: 120° to 135°	(a) CFRP bidirectional/Al 2024/CFRP bidirectional (b) Total thickness: 13.5 mm	Thrust force & torque Entry delamination Surface roughness Point angle & Helix angle	[131]
(a) Spindle speed: 1000 rev/min to 3000 rev/min (b) Feed rate: 0.02 mm/rev to 0.08 mm/rev	(a) Carbide diamond coated (b) Dry cutting	(a) CFRPT800-X850/AL7075-T651 (b)Total thickness:14.7 mm	Thrust force, Heat formation, Hole quality, Hole diameter	[90]
(a) Spindle speed: 1000 rev/min to 3000 rev/min (b) Feed rate: 0.05 mm/rev to 0.08 mm/rev	(a) Single and triple margin (b) No pecking and pecking with 2 mm retraction (c) Dry cutting	(a) Ti-6Al-4 V/CFRP/AL 7050-T7651 (b) Total thickness: 30 mm	Hole diameter, Chip formation	[109]
(a) Spindle speed: 2700 rev/min to 5900 rev/min (b) Feed rate: 0.03 mm/rev to 0.07 mm/rev	(a) CVD diamond coated drill with 25°of helix angle (b) Point angle: 90°to 130° (c) Relief angle:15°to 23° (d) Dry cutting	(a) CCF300/AL 7075-T7 (b) Total thickness: 6.17 mm	Hole diameter error, Thrust force and torque Flank wear, Surface roughness, Exit burr height, Drill geometry	[65]
(a) Spindle speed: 2020 rev/min to 2750 rev/min (b) Feed rate: 0.05 mm/rev to 0.15 mm/rev	(a) Standard twist, double cone M1 and double cone M2 (b) Dry cutting	(a) CFRP T700-M21/Al 2024 (b) Total thickness: 7.2 mm	Thrust force, Surface roughness, Delamination, Chip shape	[20]
(a) Spindle speed: 60 m/min to 120 m/min (b) Feed rate: 0.15 mm/rev to 0.3 mm/rev	(a) Double cone and flat point geometry (b) primary point angle: 130°to 140° (c) Secondary point angle: 60° and 180°	(a) CFRP/AA7010-T7451 (b) Total thickness: 16.5 mm	Hole diameter Bur formation Delamination	[39]
(a) Spindle speed: 60 m/min to 120 m/min (b) Feed rate: 0.15 mm/rev to 0.3 mm/rev	(a) CVD diamond coated drill (b) Double cone and flat point geometry (c) Primary point angle: 130° to 140° (d) Secondary point angle: 60° and 180°	(a) CFRP/AA7075/CFRP (b) Total thickness: 26.1 mm	Tool wear Hole diameter Thrust force Delamination	[132]

Table 3 (continued)

Drilling parameter	Tool & Environment	Workpiece	Findings	Author
(a) Spindle speed: 30/120/120 m/min for the Ti/CFRP/Al layers respectively (b) Feed rate: 0.05 mm/rev to 0.08 mm/rev	(a) Uncoated and TiAlN/TiN coated WC (b) Drilling strategy: pecking and without pecking	(a) Ti-6Al–4 V/CFRP/AA7050 (b) Total thickness: 30 mm	Tool life Thrust force Tool geometry	[91]
(a) Spindle speed: 1000 rev/min to 3000 rev/min (b) Feed rate: 5 mm/min to 15 mm/min	(a) Solid carbide twist drill and helical milling tool (b) drilling strategy: multistep process and helical cutting process	(a) CFRP HTS40 12K300/Al 2024-T3 (b) Total thickness: 4 mm	Hole delamination Pecking method, Roughness	[133]
(a) Cutting speed: 145 m/min (b) Feed rate: 250 mm/min	(a) WC–Co helical drill without coat (b) Helix angle 29.82 degree (c) Double point angle (118°/140°) (d) Dry machining	(a) CFRP/UNS A97075-T6 (b) Total thickness: 9.36 mm	BUL and BUE Cutting force Hole diameter	[134]
(a) Cutting speed: 85 m/min to 145 m/min (b) Feed rate: 200 mm/min to 300 mm/min	(a) WC–Co helical drill without coat (b) Helix angle 29.82° (c) Double point angle (118°/140°) (d) Dry machining	(a) CFRP/UNS A92024 (b) Total thickness: 10 mm	Diametric deviations, Surface quality, adhesive loss (using ANOVA) Hole diameter	[135]

surface also increases with the reduction in temperature, and it provides extra resistance leading to increased force levels when drilling Al panel [160, 161]. Betrolini et al. agreed with it and said that cryogenic cooling assisted drilling on CFRP/Al stacks increased the thrust force on Al panel by 20%, 27%, and 23% for feed rate of 0.05, 0.1, and 0.15 mm/rev, and when drilling the CFRP sheet, it did so by 62%, 53%, and 45% in comparison to the dry drilling approach [162]. LCO_2 is also used by some researchers as cryogenic coolant when performing CFRP/Al stack up drilling. The volumetric expansion-based CO_2 cooling process causes the liquefied pressurized stored CO_2 to cool at a temperature of − 78.5 °C just prior to the cutting zone [163]. Seeholzer et al. said that, if the prime focus is to cool the aluminum plate, it will barely be affecting the temperature of CFRP panel when supplying CO_2 cryogenic coolant from the Al plate side [157]. Kneubühler et al. mentioned that around 50% of chip breakage occur by using CO_2 cooling from the workpiece side, and as the chip advances along the chip flute, the effects of pressurized air and CO_2 cooling start to fade [163]. They further mentioned that CO_2 cooling from the tool side caused approximately 90% of chip breakage, produced the highest thrust force, and small, separated Al chips indicated that the secondary material separation was continuously achieved [163]. The shapes of the Al chips obtained by them using various cooling methods which are discussed above are shown in Fig. 13.

The minimum quantity lubrication (MQL) environment aids in the greatest force reduction by reducing friction between the machining surface and the chisel edge [164]. While the lubricant helps to disintegrate the heat from the machining region, high-pressure helps the lubricant to penetrate effectively, functioning as a chip breaker and clearing the generated chips from the cutting zone as soon as possible [157]. Meshreki et al. supported this statement by comparing the results of low pressure—high feed (LP-HF) MQL and high pressure—low feed (HP-LF) MQL cooling. They found that LP-HF MQL resulted in poor penetration of the jet, thus resulted in higher forces in all directions [155]. They further noticed that drilling in dry mode and using HP-LF MQL gave lower cutting forces in CFRP, while HP-LF MQL and flood cooling were commendable in aluminum panel as shown in Fig. 14. [155]. This difference in the force fluctuation between the layers is due to the mechanical characteristics of each layer [159]. Janakiraman et al. mentioned that the force levels during dry drilling were in-between to those under MQL and cryogenic conditions [158]. Kneubühler et al. [163] found that rare chip breakage occurs (30%) in dry drilling whereas pressurized air leads to a more frequent chip breakage (40%). This variation can be described by the added pressure that pushes the chip toward the chip flute, allowing the crack to fully propagate and increase the likelihood of subsequent material separation. Seeholzer et al. [157] also mentioned the same that chip evacuation is improved by pressurized air because, at the start, only a few chips are created, but as drilling depth increases, chips begin to accumulate. Chip evacuation keeps chips from rubbing up against the hole wall and helps expose the drilled region to cold air for better heat dissipation [164]. Chip accumulation is caused by inadequate chip transport, whereby individual chips become

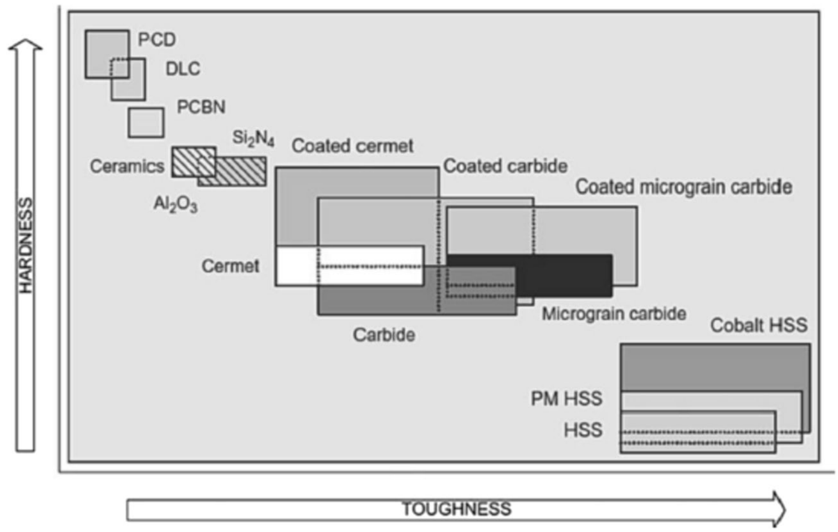

Fig. 11 Overall hardness and toughness level for well-known cutting tool materials [140]

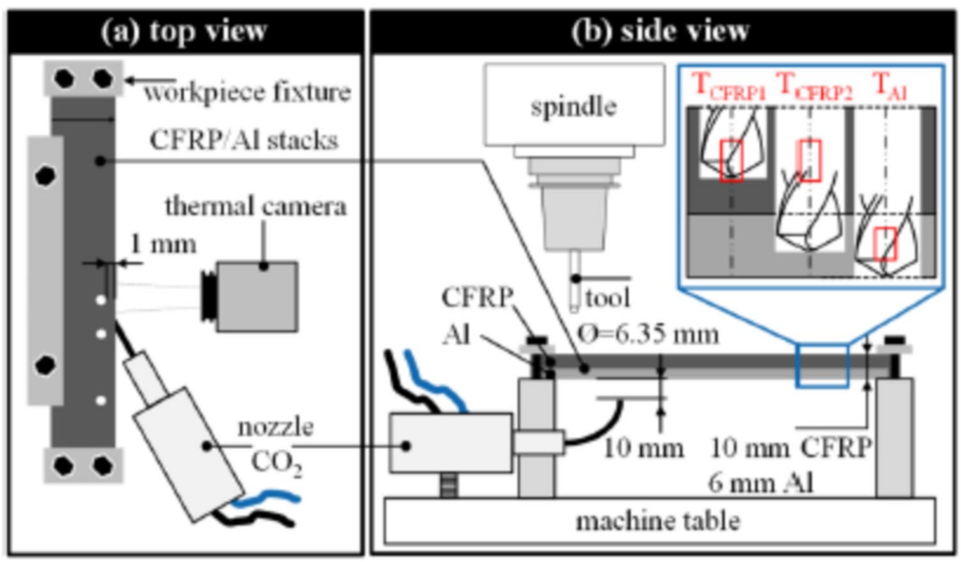

Fig. 12 Schematic illustration of the test rig: (a) top view and (b) side view [157]

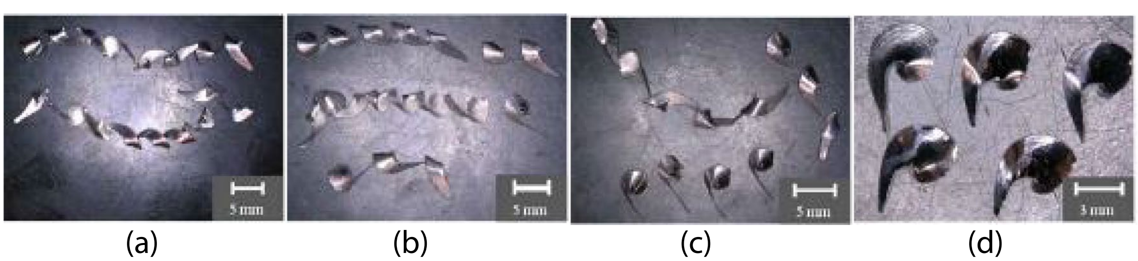

Fig. 13 Al-chips formed while using (**a**) dry cutting, (**b**) cooling with compressed air (8 bar) through the tool (**c**) liquid CO_2 (60 bar) from the work piece side (**d**) liquid CO_2 (60 bar) from tool side through the cooling channels [163]

trapped in the chip flute and subsequently squeezed at an elevated temperature [157]. Smaller chips would be formed during the machining at low temperatures, which reduces the possibility of accumulation of chips in the chip flute.

Janakiraman et al. discovered that the thrust force difference between the dry and MQL environment was minimal at higher feed rates, despite the maximum reduction in thrust force of 17.2% with the MQL environment [158]. This

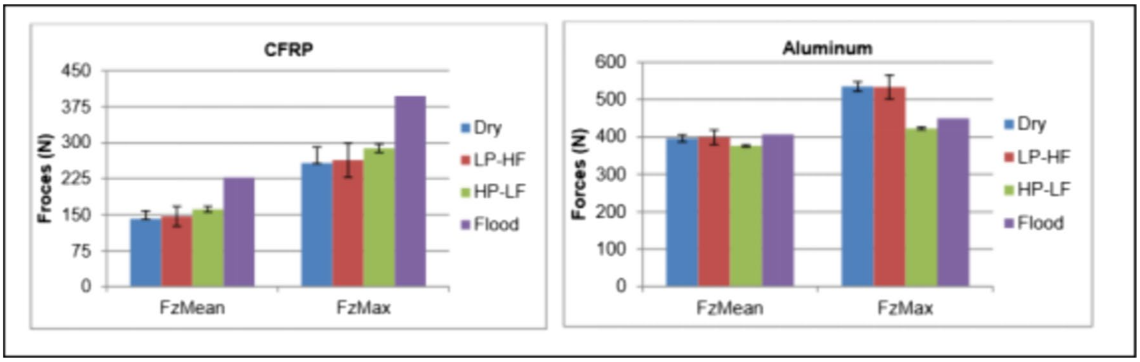

Fig. 14 Drilling thrust forces in (**a**) CFRP and (**b**) aluminum panels with different cooling methods [155]

may be because of either MQL unable to dissipate the heat produced at increased feed rates or because of the higher friction between workpiece and tool at increased feed rates [155]. The elevation in temperature resulting from friction leads to a decrease in oil's viscosity, impacting the flowability of the lubricant. This, in turn, disrupts the maintenance of a proper film, subsequently amplifying the exposure of the tool to the surface and the tool to the chip [158]. Exaggerated thrust force may also be associated with increased tool edge contact with abrasive fibers and a significant rise in hole surface resistance force [165]. However, there was also a chance that the oil coating could completely break down at high temperatures, which shows that MQL is inefficient at increased feed rates since it resembled a dry condition [166].

Shyha et al. performed cooling experiments with Ti/CFRP/Al stacks and observed that, irrespective of drill coating, the noise levels increased because of the rubbing friction between the tool and metal layers when using spray mist application and low cutting speed [167]. They stated that the life of the tool was inadequate and the maximum number of drilled holes was only about 100 when using spray mist cooling. Testing with the uncoated drill at moderate and high cutting speeds created a screaming sound with sparks which resulted in even lower tool lifetime. In the experiments performed by Shyha et al. while cutting with flood coolant, the force associated with Ti (285–600 N) was significantly greater compared to both CFRP (44–190 N) and Al (135–342 N) [167]. However, because only low concentrations of spray mist lubricant reached the Al panel, which is the bottom layer, thrust force noted in the Al layer (234–540 N) occasionally exceeded those noted in the Ti layer (239–426 N) in a spray mist environment. Their conclusions were also corroborated by the outcomes of their ANOVA analysis, which showed that feed rate significantly affects the formation of thrust force in each of the three layers, with PCR of 40%, 31%, and 20% for Ti, CFRP, and Al, respectively [167]. Generally speaking, the force levels measured during Ti drilling were about three times higher than those of CFRP and Al cutting. The lowest torque was recorded in CFRP, then in Al and Ti, which is consistent with the tendency of titanium and aluminum swarf to attach on the drill edges and lips [167].

3.4.2 Impact of cooling on hole damage

Cryogenic conditions and MQL are characterized by reduced friction, improved heat dissipation, and minor hole damage. When considering delamination, Janakiraman et al. found that delamination factor was highest under dry conditions, followed by MQL and least by cryogenic LN_2 condition [158]. Due to MQL's limited penetration and inferior cooling capacity, its effect was not as strong as LN_2's [155]. Despite the highest thrust force, using LN_2 proved to be more effective at controlling delamination than using MQL. This may be because of the enhancement of the CFRP's interlaminar shear strength at low temperatures [168]. On the other hand, Bertolini et al. and Nagaraj et al. noted that regardless of feed rate, significant exit delamination only happened when cutting trials were performed on CFRP/Al stack under LN_2 cryogenic drilling as opposed to dry and ultrasonic vibration assisted drilling [162, 169]. In contrast, under cryogenic and MQL conditions, Janakiraman et al. found that the highest delamination occurred by increasing the feed rate at a constant cutting speed and not because of the variations in the oil flow rate [158]. This phenomenon is particularly notable because a larger thrust force corresponds to an enlarged exit delamination and the deflection of the final ply of the fiber metal laminate (FML) intersects a broader zone with increased force [170]. Janakiraman et al. further mentioned that the delamination factor rises at a cutting speed of 125 m/min in a dry environment before decreasing at a cutting speed of 150 m/min [158]. This decrease can be caused by thermal softening occurred from higher frictional heat produced throughout the process thus ensuing drop in cutting forces [2]. In general, the lack of adequate cooling at higher temperatures promotes thermal softening since the material exhibits less internal deformation resistance [163]. The application of cryogenic cooling stiffens the epoxy matrix which may enhance the rigidity of the fibers causing shear rupture and brittle fracture behavior of the workpiece material rather than bending and tearing resulting in increased process forces [72]. Meshreki et al. said that, while holes free from entry delamination were generated by dry and flood conditions, the holes drilled with MQL (LP-HF) and (HP-LF) had delamination of 1.167 mm (24% of the diameter) and 0.915 mm (19% of the diameter) [155]. This could be due to higher horizontal forces in the case of MQL compared to dry and flood modes [99].

Janakiraman et al. noted that under cryogenic conditions, larger cutting speed and smaller feed rate revealed the superior surface finish. Additionally, though drilling under cryogenic and MQL conditions showed a similar pattern but with a comparatively lower increase, drilling under dry conditions showed a substantial growth in surface roughness (R_a) depending on the feed rate [158]. They further mentioned that variations in cutting speed in dry conditions had the greatest impact on roughness, whereas feed rate predominated in MQL conditions. The lower temperature in the cutting region caused by MQL may be responsible for the improved hole quality since it averts the chips from fusing to the drill bit and harming the hole surface [158]. Additionally, it was discovered that in cryogenic drilling environments, as compared to MQL and dry environments, the influence of feed rate on surface roughness was marginal. This is due to the laminate's constituent composite layers undergoing a ductile–brittle transition at cryogenic temperature [158]. Moreover, Giasin et al. mentioned that, as a result of the laminate's lower compressive stresses resulting from carbon, glass fiber, and aluminum sheets' minor differences in thermal expansion under cryogenic environment, the plies were substantially less distorted, which improved the surface smoothness [54]. The enhanced hole quality in cryogenic conditions may also be attributed to the minimum build-up edge (BUE) that developed on the drill bit as a result of the cushioning effect formed by the efficient dispersion of gaseous nitrogen coolant into the tool-chip interface [171]. Zitoune et al. also found that the fusion of metal chips to the drill bit's cutting edges may be the cause of imprecise surface roughness [45]. BUE was reported to form mostly on the drill margins and the principal cutting lips in spray mist application trials, according to Shyha et al. [167]. This was most likely brought on by the spray mist lubricant not being applied enough to the machining area, particularly as the drill bit penetrated deeper into the bottom aluminum layer of the stack. In contrary to all the above observations, Meshreki et al. mentioned that dry drilling gave better

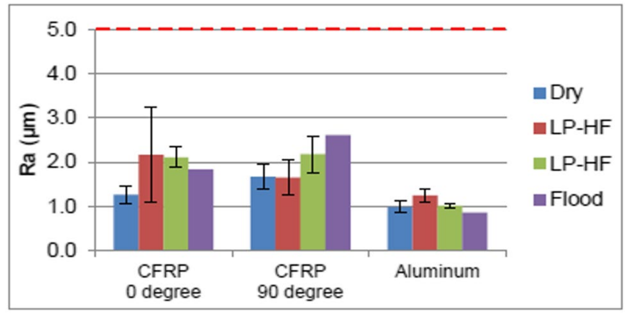

Fig. 15 Surface roughness values for CFRP and aluminum at different cooling methods [155]

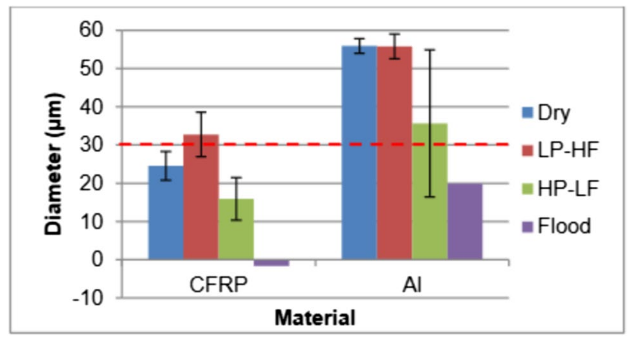

Fig. 16 Diameter error values in CFRP and aluminum for different cooling modes [155]

surface roughness than the holes obtained in all kinds of cooling for both CFRP and Al panels as shown in Fig. 15. It should also be noted that the surface roughness of all the tested cooling modes fell within 3 µm and did not follow a noticeable trend [155]. Among all the samples, the surface roughness is higher in CFRP compared to Al due to the heterogeneity of CFRP [155]. It is also supported by Zitoune et al. that the CFRP/GFRP interface's average surface roughness is significantly larger than that of the metallic alloy panel [45].

When considering diameter variations, Meshreki et al. found that flood cooling gave the lowest diameter errors followed by HP-LF MQL as shown in Fig. 16 [155]. They further mentioned that, in CFRP panel, the lowest circularity error was obtained under flood cooling, while in aluminum panel it was LP-HF MQL and then HP-LF MQL that offered the best results, but all the circularity errors were below 25 µm [155]. According to Shyha et al., most of the holes produced on multi-layer stacks drilling under wet drilling were small, and the overall tendency is the drop in diameter with increase in number of holes [46]. Such phenomenon can be explained by material loss brought on by tool wear that grows with the number of holes. According to Kneubuhler et al., there was no discernible variation in the location of the crack's initiation regardless of the cooling method [163]. With regard to the location of the crack initiation, it is therefore considered that the process parameters and the tool geometry have a larger impact than the cooling techniques.

According to Shyha et al., variances in hole roundness for the Ti, CFRP, and Al layers in a Ti/CFRP/Al stack panel drilling were up to 78, 39, and 53 µm, respectively, under wet conditions, while cylindricity error varied from 23 to 120 µm for the overall stack. This variation increased for spray mist environment up to an average of 170 µm [46]. Table 4 presents the researches conducted to investigate the impact of cooling strategies on stack up drilling. Researchers tried various cooling environments by changing the types of coolants, air pressure, coolant flow direction, etc., to determine the best cooling strategy. Most of their focus was centered on improving hole quality by mitigating thrust force and improving the chip evacuation methods. Along with all the abovementioned strategies, application of coating to drill bit also improves the hole quality of single shot drilling of stack up materials, and which will be discussed in the next section.

3.5 Coating applications

The extent to which coated drill bits establish tribological relationship between tool-composite component and tool-metallic component is the major factor in their desirability of selection for stack material drilling [173, 174]. These interactions may be utilized to forecast surface quality and the frequency of delamination in composite material drilling [175]. Production companies mainly use inorganic compounds to coat drilling tools either through physical vapor deposition (PVD) [176, 177] or chemical vapor deposition (CVD) [136]. A sample set up for PVD coating and SEM image of the cross-section of coated tool is shown in Fig. 17. The PVD laborious coating often improves machining efficiency and tool life [176, 177].

3.5.1 Impact of coating on thrust force

Thrust force can be affected by numerous factors, like tool geometry, cutting parameters, tool material, tool coating, lubrication and cooling technique, and workpiece material

Table 4 Impact of cooling on CFRP/Al stack material drilling

Workpiece	Tool	Cooling Strategy	Findings	Author
CFRP/Al7175	diamond-coated cemented carbide spiral drills	C0: Uncooled; C1: Compressed air (6 bar) cooling through the tool C2: Cryogenic CO2 cooling from Al side (– 80 °C, 25 kg/hr) C3: Combination of CS1 and CS2	1. Chip evacuation 2. Cooling of Al and CFRP stacks	[157]
CFRP/Al 7010-T651	WC/Co, TiAlCrN coating	Coolant – Accu-Lube® LB-4000 Coolant flow – 1 l/h	1. Hole damage	[172]
CFRP/Al	2-flute uncoated drill	Dry Drilling (MQL) with low pressure (< 1.5 bar) and high flow rate (400 ml/hr) MQL with high pressure (4.25 bars) and low flow rate (10 ml/hr), Flood cooling	1. Cutting force 2. Temperature 3. Diameter error 4. Concentricity	[155]
CFRP/Al7075	ArCr-based coated cemented carbide drill; workpiece rotates, tool linear feed	C0 – Dry cutting C1 – Cooling with compressed air (8 bar) through the tool C2 – Liquid CO2 (60 bar) from the work piece side C3 – Liquid CO2 (60 bar) from tool side through the cooling channels	1.Thrust force 2. Crack formation 3. Chip breakage 4. Chip evacuation	[163]
CFRP/GFRP/Al	Uncoated WC twist drills	Dry cutting (MQL) cooling Cryogenic cooling	1. Thrust force 2. Delamination 3. Surface finish	[158]
Ti-6Al4V/CFRP/AA7050	CVD diamond coated WC, C7 coated WC and uncoated WC	Wet & Spray mist pump pressure of 70 bar and flow rate of 15 ml/min; Feed – 0.05, 0.1 & 0.15 mm/rev; Speed (rpm) – (1000/2000), (2000/4000), (3000/6000),	1. Thrust force	[167]

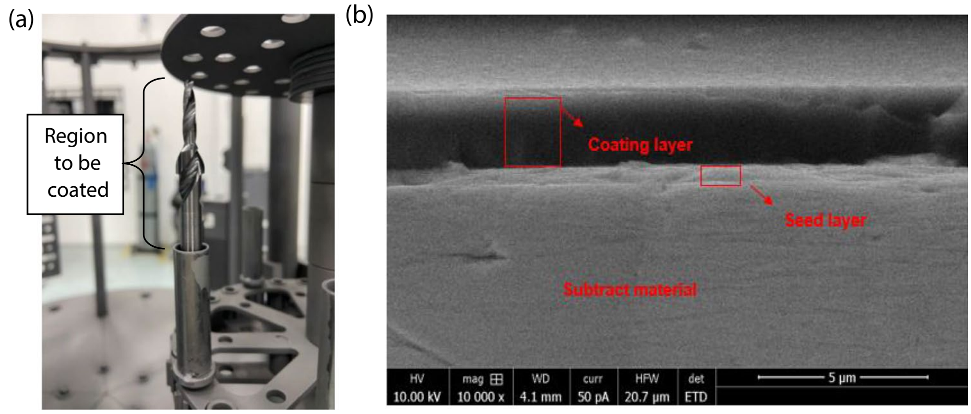

Fig. 17 **a** Drill bit set up for PVD coating process. **b** SEM observation of the formation of ta-C coating and seed layer [178]

[132]. Zhong et al., when comparing the thrust force while drilling CFRP/Al/CFRP stack, showed that, whatever the feed rate is, as cutting speed increases, the maximum thrust force with the uncoated tool is higher than with the TiAlN-coated tool as shown in Fig. 18 [179]. They further stated that the maximum thrust forces with the later are 40–50 N larger than with the former, because TiAlN coating provides wear resistance, high hardness, and chemical stability [179]. Additionally, the opposite results were also attained with low feed rate and low speed [179]. When drilling aluminum panel with an uncoated tool while increasing the feed, Zitoune et al. saw a minor reduction in thrust force (about 5%), and suggested that this might be due to the increased drilling temperature along with the feed and therefore the softening of the workpiece [45]. This reduction was estimated to be 10% while drilling CFRP. Because nano-coating reduce the friction between the tool and the machined surface of the hole and between the tool and the chip, it may be anticipated that an uncoated tool produces more heat during machining than a tool that has been coated with nanoparticles. Additionally, nano-coating enhances the tool's thermal conductivity [45]. The average thrust force of the coated drill is 30 to 50% higher than the thrust forces of the uncoated drills during the first hole when the drills are new, according to Montoya et al. as can be seen from Fig. 19. This is mainly because of the sharpness of the cutting edge [88]. The coating thickness is the cause of this variation in cutting-edge sharpness. Their tool's cutting-edge radius was 9 µm for uncoated tool and 11 µm for tools coated with TiAlCrN and AlTiSiN-G while 15 µm for diamond coated tool. Kuo et al. conducted research on Ti6Al4V/CFRP/AA7050 stack with WC twist drills coated with TiN and TiAlN and found a similar trend [91]. They discovered that, in majority of the situations, coated drills increased thrust force by 12–18%, likely as the outcome of higher cutting-edge radius (33 µm) and consequently reduced sharpness compared to uncoated tools (cutting edge radius of 23 µm). It is important to consider cutting edge radius because Franke mentioned that the separation of fibers is greatly hampered if the fiber diameter is smaller than the cutting-edge radius [180].

Montoya et al. mentioned that drilling of Al panel at designed cutting parameters produces a larger maximum

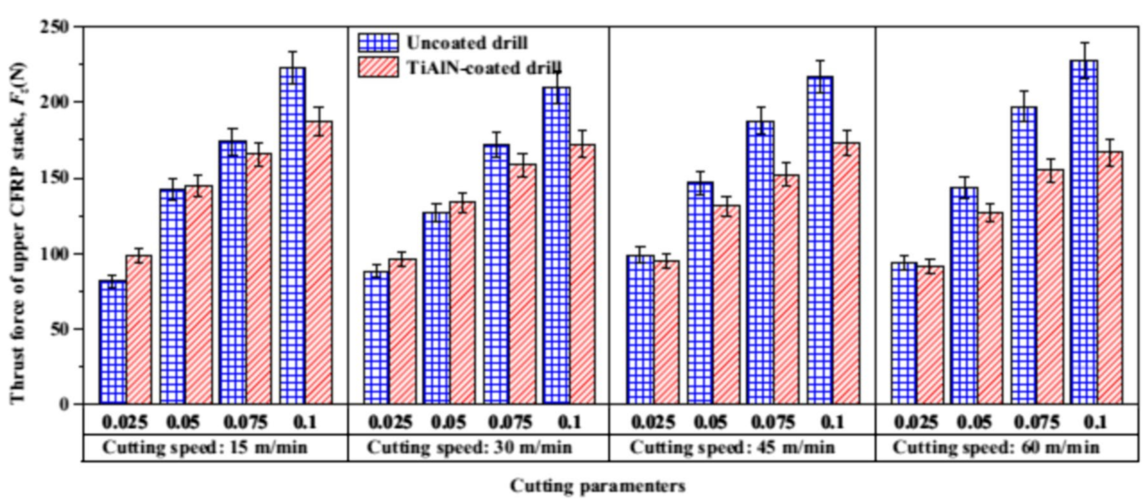

Fig. 18 Thrust force magnitudes in upper CFRP stack [179]

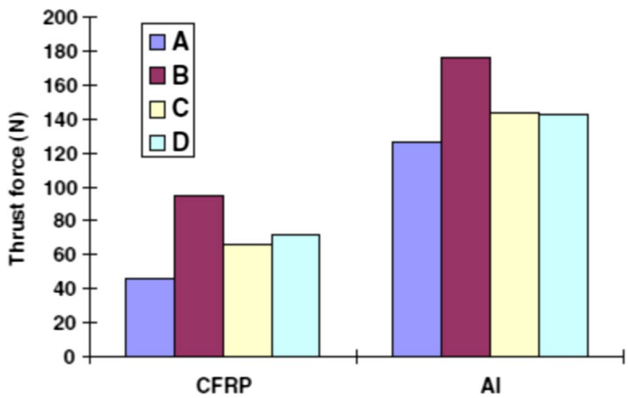

Fig. 19 Average thrust force on the first hole: **A** uncoated, (**B**) diamond coated, (**C**) TiAlCrN coated, (**D**) AlTiSiN-G coated [88]

thrust force than drilling CFRP panel [88] and it is supported by some other researchers [45, 179]. Zitoune et al. and Meshreki et al. further mentioned that when drilling aluminum panel, it was discovered that the thrust force was two to three times greater than when drilling composite material as shown in Fig. 20 [45, 155]. But according to Brinksmeyer et al., the thrust forces were higher in CFRP than Al with the drill that has a larger diameter of 16 mm [139]. The different cutting pressures created by the drill and the materials of the workpiece can account for this discrepancy in forces [119]. When drilling CFRP/Al stacks, the use of diamond coating can lower the force by 65% and 35% in CFRP and Al, respectively, by reducing wear [88].

Zhong et al. discovered that the higher influence on thrust force is from feed rate compared to speed while machining CFRP/Al/CFRP stack with uncoated and TiAlN coated drill bits as shown in Fig. 18 [179]. They found through ANOVA analysis that feed rate (93.8–98.79%) and cutting speed (1.21%–6.29) have an impact on the maximum thrust force. Zitoune et al. also found this fact experimentally that, for both CFRP and Al panels in a stack, the thrust force is directly proportional to the feed rate, and mostly unaffected by spindle speed [45]. They observed an increase of 72% and 92% from first hole to 70th hole in thrust force while drilling CFRP/Al stack with coated and uncoated drills respectively. The increased wear on the uncoated tool is the cause of this rise compared to the coated one [45]. Irrespective of the type of tool used, an increase of 11% in thrust force has been seen in aluminum panel from the first hole to the final (70th) hole. The main type of wear that is seen when drilling aluminum or isotropic materials is flank wear. It may be inferred that flank wear is minimal because there is very little difference in the thrust force on the aluminum between the first and last holes [45].

According to Kuo et al., despite having high thrust force, coated drills have up to 10% lower torque values, which is consistent with the increased wear resistance provided by TiAlN/TiN coating at the corners [91]. They further mentioned that running at higher feed rate of 0.08 mm/rev will reduce the wear rate of the drill by up to 28%, which was most probably caused by a shorter contact time between the workpiece and tool demonstrating the importance of feed rate. Additionally, ANOVA calculations revealed that drill wear was significantly influenced by both tool coating and feed rate, with the former having a partial correlation regression (PCR) of 78.4% [91].

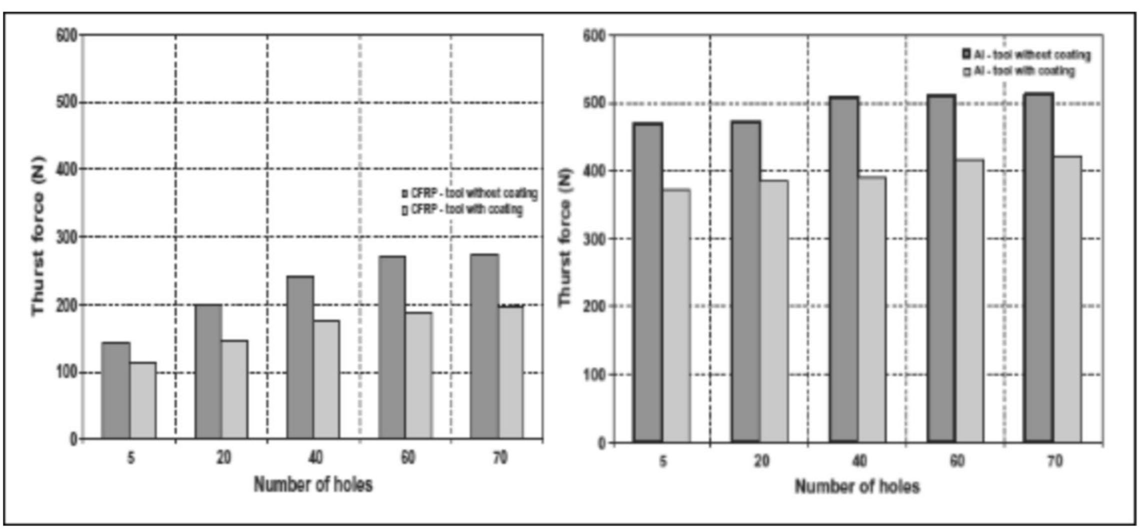

Fig. 20 Influence of the number of holes drilled on the thrust force. **a** Thrust forces measured in the CFRP and (**b**) thrust forces measured in the aluminum [45]

3.5.2 Impact of coating on hole damage

Number of scholars have explored with various coatings like TiN, TiAlN, TiAlCrN, TiSiN, DLC, TiAlCr/TiSi, TiAlN/AlN, AlTiSiN-G, nc-CrAlN/a-Si_3N_4, and TiB_2 and reported the output with regard to hole quality as follows. Brinksmeier and Janssen obtained close diameter tolerances when drilling with TiB_2-coated tool when compared to diamond coated and uncoated tool while drilling $AlCuMg_2$/CFRP/TiAl6V4 [48]. Montoya et al. mentioned that the relationship between hole diameter and number of holes is largely consistent within the range of 5.965–5.98 mm for uncoated and diamond coated tools compared to 5.96–5.995 mm in TiAlCrN and 5.955–5.98 mm in AlTiSiN-G coated tools while drilling CFRP/Al stacks [88]. The experiment with TiAlCrN and AlTiSiN-G was stopped before reaching 80 holes due to coating breakage [88]. Though the diameter difference between 1st and 250th hole is less than 15 μm for uncoated and diamond coated tool as observed by Benezech et al., uncoated tool shows a slightly increasing pattern of diameter and diamond coated tool shows slightly decreasing pattern with increasing number of holes [111]. This could be because of coating degradation in diamond coated tool and increasing wear in uncoated tool [132]. D'Orazio et al. also mentioned that the diameter reduces with increase in the number of holes while drilling CFRP/AA7075/CFRP by DLC and TiAlN coated drills under dry cutting condition [132]. As can be seen from Fig. 21, first 60 holes out of 170 total holes drilled by TiAlN coated drill were oversized than the drill bit ($d = 6.8$ mm) while all the holes drilled by DLC was smaller than the drill bit diameter. Additionally, Shyha et al. demonstrated that, when performing wet cutting on multi-layer stacks, the majority of the holes created were smaller in size [46]. Kuo et al. while drilling Ti/CFRP/Al stack mentioned that, in comparison to the uncoated tools, the holes made by the TiAlN/TiN-coated drills at test termination (90–148 holes) shown greater precision with regard to diameter with maximum deviations of 0.02 mm from the nominal value of 6.35 mm (180 holes) [91]. Also, holes drilled by coated tool shows consistent diameters with increased feed rate while that of the uncoated tool shows increased diameter with increased feed rate. Additionally, it was discovered that tool coating, with PCR of 64.5% and 57.5%, was the main variable determining hole diameter in both CFRP and Ti layers. According to D'orazio et al., at 170th hole, the diameter difference between the drills with DLC coating and TiAlN coating approaches a value of about 32 μm and about 58 μm, respectively, due to tool wear development [132]. It is because the TiAlN-coated tool exhibit increased tool wear compared to DLC-coated tool.

When considering hole cylindricity, Kuo et al. found that the uncoated drills gave hole cylindricity error of maximum 150 μm while TiAlN/TiN-coated tools gave maximum of 100 μm [91]. They added that despite having lower flank wear levels, poor cylindricity was visible across the holes drilled with the uncoated tool. Tool coating has an impact on delamination as demonstrated by D'Orazio et al. since the wear-free TiAlN-coated tool produced delamination factor (DF) value which is nearly double that of by the DLC-coated tool [132]. Additionally, it was noted that throughout the experiment, DLC-coated drill produced a lower delamination factor (DF) value than the TiAlN-coated tool, regardless of the number of holes. They also demonstrated that for both TiAlN- and DLC-coated tools with identical pattern of holes, the delamination factor monotonically increases. Zhong et al. discovered that the delamination factor at the hole entry achieved with an uncoated drill bit is larger than that obtained with

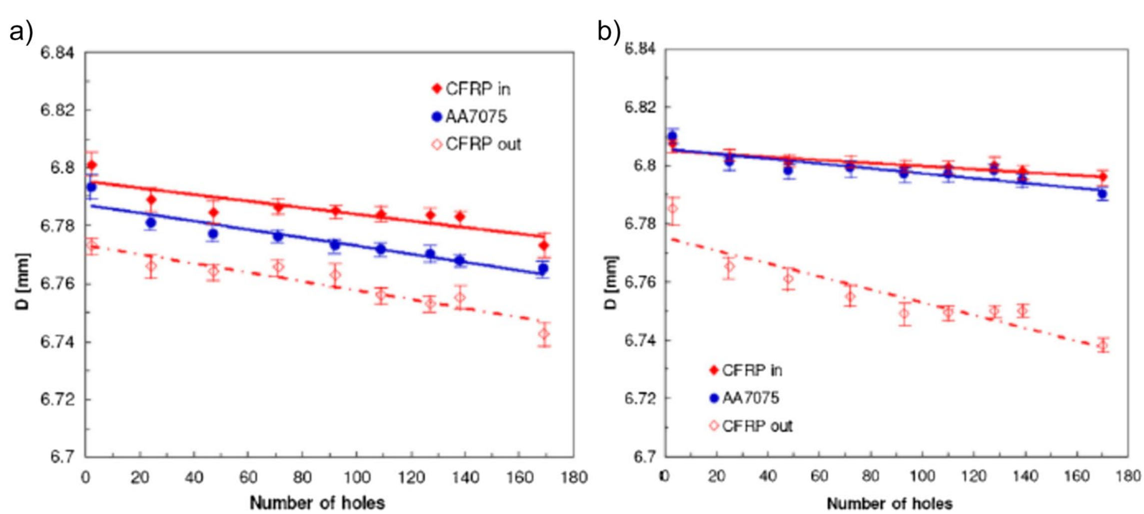

Fig. 21 Evolution of hole diameter with number of holes using (**a**) DLC-coated drill and (**b**) TiAlN-coated drill [132]

a TiAlN-coated drill with the same cutting speed and feed rate [179], but TiAlN-coated drills have a delamination factor at the hole exit that is around three times smaller than that of uncoated drills as shown in Fig. 22 [179]. This might be as a result of the TiAlN coating's high hardness. Elevated hardness could disperse and reduce thrust force. Reducing the thrust force can effectively lead to a lower delamination factor, which will enhance the hole's machining quality. Additionally, Kuo et al. and Karpat et al. noted that reducing flank wear reduced delamination, and the best tools for this are those with CVD diamond coating [91, 181]. Contrarily, Brinksmeier and Janssen state that using coated tools has no effect on CFRP for the damages occurred due to erosion phenomenon between the generated sharp metal chips and the CFRP [48]. Montoya et al. also mentioned the CFRP damage at the hole entrance starting with the first hole regardless of whether uncoated or diamond-coated drill is used [88]. Therefore, it can also be deduced that this phenomenon may be induced by the tool geometry [132, 182] in which the initial layers of the composite material are pulled off by the drill flute in addition to tool wear [88]. Few researchers tried with adding dopant/seed layer before adding coating layer to tool while performing single-shot drilling of CFRP/Al stack panel. Prajapati et al. mentioned that adding Cr to TiAlN leads to excellent performance [137]. Mathavan et al. also mentioned that tetrahedral amorphous carbon (ta-C) coating reduced the delamination factor by reducing the tool wear due to the high bonding strength and high hardness of this coating type. They noted also that the addition of Cr dopant to ta-C coating did not yield improved results, and this was attributed to two factors. Firstly, the chromium dopant added tetrahedral amorphous carbon (ta-C:Cr) coated tool experienced faster degradation because of the peel-off of the coating, as the bond strength of the coating was minimal compared to dopant-less ta-C coating. Secondly, the ta-C:Cr coating showed the lowest hardness compared to dopant-less ta-C coating, preventing effective spread and reduction of thrust force, ultimately leading to a higher delamination factor [178].

According to a study by Zitoune et al., using a tool with a nc-CrAlN/a-Si3N4 nanocoating improves the surface polish on Al and CFRP holes [45]. This variation is primarily attributable to the tool polishing, particularly before PVD coating for improved bonding of the nanocrystalline layer. According to literature, the essential specification for the hole surface roughness of individual CFRP and aluminum alloy must be less than 3.2 μm and 1.6 μm, respectively [65]. The hole surface roughness obtained by Montoya et al. for Al was below 1.6 μm throughout the experiment (250 holes) for holes machined by both uncoated and diamond-coated tools, but in CFRP, it exceeds 3.2 μm at around 80 holes by the uncoated tool, while the diamond-coated one stay within the limit [88]. This is a result of rapid development of wear experienced with uncoated tool. The drill cannot cut the carbon fibers when the drill bit's cutting-edge sharpness is too low. Higher rubbing of the tool with workpiece material occurred as the periphery corner wore down, causing matrix cracking, delamination, voids, fiber protrusion, and adhered resin on the drilled surface [91]. Diamond-coated tools have a mild evolution of the cutting-edge profile, which results in low hole surface roughness and strong stability [88]. Zhong et al. also discovered that, while drilling CFRP/Al panel, using an uncoated drill produces more surface cavities on the hole wall surface than using a TiAlN-coated drill (Fig. 23) [179]. The TiAlN-coated drill's increased hardness, which reduces its wear, thus, will create less thrust force, and in turn will reduce mechanical damage. However, experimental work of Kalidas et al. demonstrates that the surface roughness of the hole created at the aluminum part did not seem

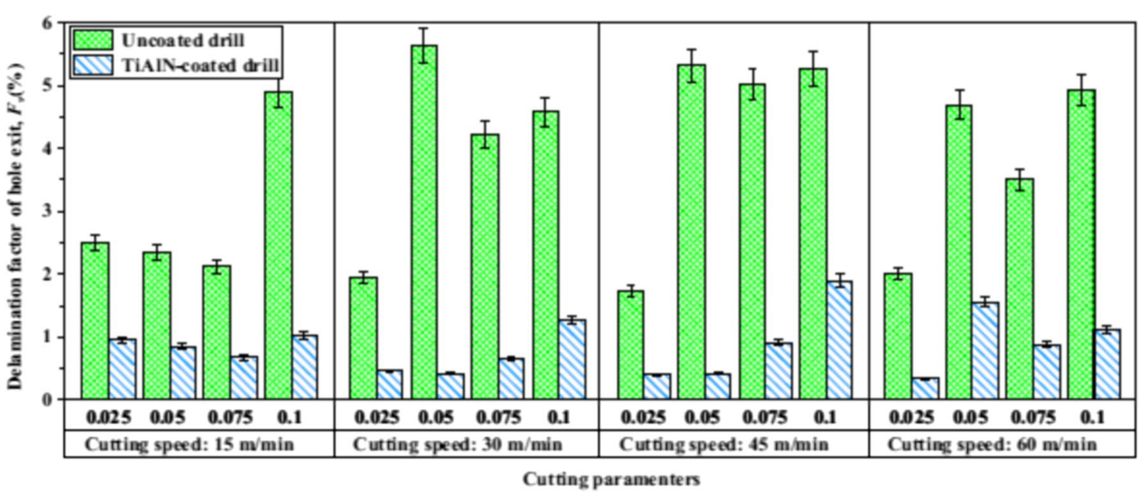

Fig. 22 Delamination factor results for holes exit [179]

to be affected by the application of coatings (TiAlN, TiAlN/AlN, and MoS2) [183]. Kuo et al. also did not obtain any significant improvement in hole surface roughness while drilling Ti/CFRP/Al with TiAlN/TiN-coated drill when compared to uncoated tool [91].

Studies have shown that drill bits with a TiAlN coating exhibit improved performance with regard to burr height compared to uncoated drills. These coated drill bits are able to keep the burr height below 80 µm, therefore eliminating the need for the deburring procedure [184]. This observation was also supported by Kuo et al. when they drilled Ti/CFRP/Al stacks using a tool coated with TiAlN/TiN [91]. They observed that the drill with a coating had a maximum burr height of 150 µm, but the uncoated drill had a maximum burr height of 200 µm. The discrepancy was ascribed to the diminished buildup of the aluminum layer at the cutting edge. The coating prevented the aluminum chip from permanently adhering to the tool surface, hence preventing the formation of a buildup layer or edge (BUL or BUE) [184]. The burr height will increase if there is greater fusion at the tool's cutting edges because the drill bit will tend to extrude rather than cut to finish the drilling operation [134]. Mathavan et al. mentioned that ta-C:Cr-coated tool formed minimum burr height of 96.4 µm compared to ta-C-coated tool 126.75 µm [178]. They added that as the ta-C:Cr-coated tool produced the minimum coefficient of friction (COF), that is the reason why there was less burr height creation. Reduced coefficient of friction causes the tool to rub against the workpiece surface less, which lowers the generation of temperature. This, in turn, causes low ductility at the hole edge, which ultimately leads to reduced burr formation. The largest burr height was created by the ta-C-coated tool, which also has the highest COF [178].

Table 5 summarizes various studies that have been conducted on the application of different coatings to drill bits while drilling stack up materials. These coatings include TiN, TiAlN, DLC, TiAlCrN, AlTiSiN-G, TiSiN, TiAlCr/TiSi, TiAlN/AlN, nc-CrAlN/a-Si_3N_4, and TiB_2. The table shows that some coatings yield better results than an uncoated tool, while others did not. The quality of the hole improvement depends on the hardness of the coating and its bond strength with the tool. Furthermore, the authors took into consideration the enhancement of tool life when selecting a coating for this application.

The hole quality can be improved by either one or combination of the abovementioned methods in Sect. 3. Once the quality is improved, it is essential to measure and enumerate it to compare. The hole quality can be quantified in terms of certain parameters as mentioned in the next section. Several equations can be used to measure each quality parameter of drilled holes.

4 Performance measurements of hole quality

A drilled hole's diameter variation between materials, roundness or circularity, hole wall surface roughness, burr height development, and delamination can all be used to characterize a hole's quality in aircraft assembly process [116]. These characters must be taken seriously and monitored in accordance with consumer needs. Poor hole surface roughness during installation could lead to stress buildup that weakens the rivet joint [65]. Additionally, the assembly process will be hampered by a significant diameter difference between the materials for stacking and the heights formed by the burrs, which will raise the amount of scrap panel [116]. This will result in the end-product and does not conform with customer specified limit.

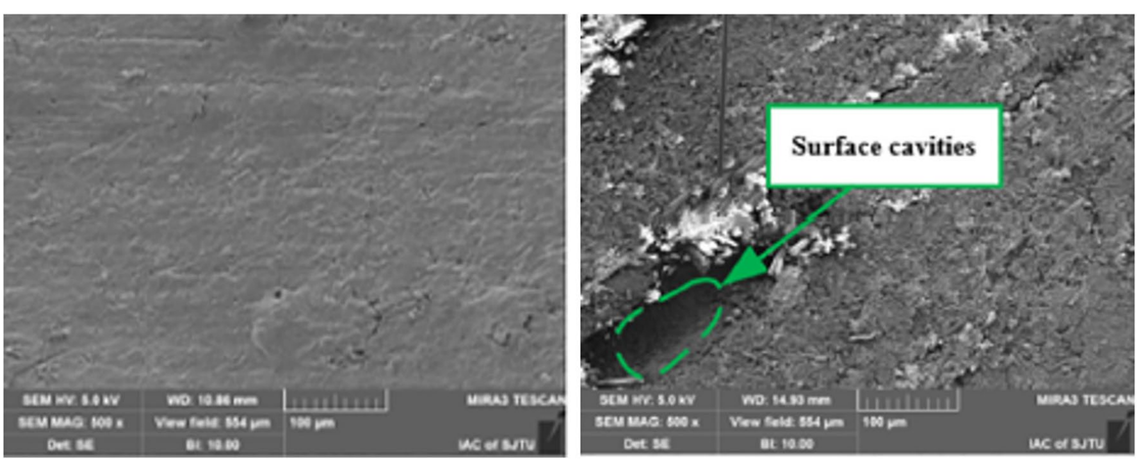

Fig. 23 SEM images showing machined surface quality of the 16th hole at × 500 with (**a**) TiAlN-coated drill and (**b**) uncoated drill [179]

Table 5 Impact of coating on single shot drilling of CFRP/aluminum stacked up materials

Workpiece	Tool	Coating	Parameters	Finding	Author
Ti6Al4V/CFRP/AA7050	WC twist drills	PVD coated TiAlN/TiN, uncoated	0.05 & 0.08 mm/rev	1. Tool life 2. Hole diameter accuracy	[91]
Ti-6Al-4 V/CFRP/AA-7050	WC twist drills	DLC and CVD coated diamond	0.08 & 0.15 mm/rev	1. Diameter of holes 2. Surface roughness 3. Burr height 4. Tool wear	[97]
Ti-6Al–4 V/CFRP/AA7050	WC drills	CVD diamond coated, C7 coated, uncoated	Feed—0.05, 0.1 & 0.15 mm/rev Speed – rev/min (1000/2000), (2000/4000), (3000/6000)	1.Tool life 2.Thrust force	[167]
CFRP/Al 7010	Standard twist drill	Diamond, TiAlCrN, AlTiSiN-G coated and uncoated	Speed-55 m/min (3000 rev/min), Feed-0.04 mm/rev, Feed rate—120 mm/min, MQL – 16 mm/min	1. Flank wear 2. Thrust forces 3. Tool failure 4. Diameter of the hole 5. Hole surface roughness	[88]
CFRP/Al 2024	Micro grain carbide	PVD coated nc-CrAlN/a-Si_3N_4 (Tripple Alwin)	Spindle speed (rev/min) 1050, 2020, 2750 Feed- mm/rev: 0.05, 0.1, 0.15	1. Surface roughness 2. Thrust force	[45]
CFRP/Al 2024/CFRP	Standard twist Drill	Uncoated and TiAlN coated	Speed 15,30, 45, 60 m/min; Spindle speed 752, 1504, 2256, 3009 rev/min; feed—0.025, 0.05, 0.075, 0.01 mm/rev	1. Hardness of the coating 2. Adhesion of Al 3. Delamination factors 4. Thrust forces 5. Surface cavities	[179]
CFRP/Al7075/CFRP	Standard twist Drill	TiAlN, DLC coated	Different cutting speed and feed for both coatings	1. Tool wear 2. The delamination factor	[132]
T800/X850 CFRP and 7075-T651 Al	Drill with double point angle	Diamond coated	Spindle speed, (rev/min) 1000, 2000 3000 Feed rate, (mm/rev) 0.02 0.04 0.06 0.08	1. Thrust forces 2. Drilling temperature 3. Diameter of the hole 4. Hole surface roughness	[90]
Ti-6Al–4 V/CFRP/Al-7050-T651	WC drill	Uncoated, C7 coated (Si_3N_4) and CVD diamond coated	Spindle speed 20/40 40/80 60/120 (m/min) Feed rate, (mm/rev) 0.05 0.10 0.15	1. Diameter of holes 2. Surface roughness 3. Burr height 4. Hole circularity 5. Hole cylindricity 6. Delamination	[46]

4.1 Hole diameter error between stacked materials

The ability to create holes with tight tolerances will depend on a number of factors, such as the size and rigidity of the cutting tool and the mechanical characteristics of the material, such as its conductivity, hardness, and coefficient of thermal expansion. Riveting and bolting in aircraft components often call for close tolerances around 25 µm [185]. Specified hole tolerances for aerospace applications are diameter difference of 30 µm or less in material stacks consisting of composites and aluminum or titanium alloys [37, 48]. The ISO 286 standard's H7 hole tolerance of ± 12 µm fit is typically required for drilling of composite metal stack materials. Greater tolerances, such as H8 (18 µm) or H9 (30 µm), were allowed to be used while drilling stacks because H7 tolerances were difficult to achieve. The tolerance for the drilled hole in a stack of composite metal, according to Sandvik Coromant tool manufacturers, may range from ± 20 to ± 40 µm [186].

The issue of different diameters between the materials is brought about by various material characteristics, particularly the materials' varying elastic moduli [187, 188]. The variation in elastic deformations arising from the distinct elastic moduli of AA7075 (E_{AA7075} = 70.6 GPa) and CFRP (E_{CFRP} = 53 GPa) may contribute to the disparity in hole diameter between the aluminum and CFRP layers. [132]. If the hole in one of the materials of the stack is too small (tool diameter > hole diameter) or too large (tool diameter < hole diameter), a rectification method must be used, which often intensify the assembly process's expense and time. Utilizing an oversized hole for material assembly may lead to loosen fitting and potential bearing failure. Conversely, connecting an undersized hole with a rivet or screw can generate pressures along the hole walls, resulting in the start and progression of cracks until component failure occurs [189].

Due to the tendency of composite fibers to contract during the drilling process, [39, 190, 191] and lubrication condition during the drilling process [88], the composite plate typically measures less size than metal parts (such as titanium or aluminum). During dry drilling on metallic panel of CFRP/Al stack, the increased temperature during the operation caused an expansion in the hole diameter due to thermal expansion [192]. Therefore, if the machining is performed in a dry condition, the aforementioned situation can easily develop during drilling [46]. Additionally, it is also possible for the CFRP hole diameter to be greater than the diameter of the Al alloy [88, 90]. According to D'Orazio et al., for both DLC and TiAlN coated tools, the AA7075 plate's hole diameter (D_{AA7075}) lies between those obtained in CFRP layers, with the entry hole exhibiting the maximum diameter (D_{CFRPin}) and the exit hole exhibiting the minimum diameter ($D_{CFRPout}$) [132]. Such discrepancy is also identified with CVD diamond coated WC drills by Shyha et al. [46]. The principal cause of the highest D_{CFRPin} value is the rubbing of the aluminum chips on the hole wall surface by the rotation of the drill [48] and most of the time it is continuous chips that cause this effect. Constant chipping increases the chance of chip blockage, which results in hot, sharp pieces that cannot be easily removed from the hole and twist along the drill's body, increase CFRP hole dimension, and degrade the CFRP panel's surface finish [80, 139]. The enhancement in drill bit direction with increased hole depth is mostly responsible for the least value of $D_{CFRPout}$ and increased hole accuracy [132]. Also, the top layer of the CFRP deforms more thermally than the bottom layer, resulting in a smaller exit hole than the entry hole diameter [132]. This is because the drilling temperature recorded in the top layer is higher than that in the bottom layer, and the reason for this phenomenon according to Wang et al. is that the dynamometer's supporting surface and the bottom CFRP layer transfer heat more effectively from the bottom of the stack panel [90].

The hole diameter inaccuracy for each panel as well as between the laminates can be calculated using the following formulas [193];

$$\varepsilon_{cfrp} = d_{m1} - d_{nom1} \tag{1}$$

$$\varepsilon_{Al} = d_{m2} - d_{nom2} \tag{2}$$

$$\varepsilon_{cfrp/Al} = d_{m1} - d_{m2} \tag{3}$$

where ε_{cfrp} is the error of CFRP panel, ε_{Al} is the error of Al panel, $\varepsilon_{cfrp/Al}$ is the difference in diameter between stack laminates, d_{m1} and d_{m2} are the measured diameters of CFRP and Al panels, and d_{nom1} and d_{nom2} are the nominal diameters of CFRP and Al panels, respectively [4].

4.2 Hole surface roughness

When considering the roughness produced in CFRP and Al panels, the roughness observed in CFRP holes were much greater than that observed in aluminum holes [45, 88, 148] as shown in Fig. 24. This can be because of the heterogeneity of composite materials, high drilling temperatures [90], and the impact of carbon fiber orientation with respect to cutting speed [45]. Previous researches have demonstrated that the method of material removal varies depending on the cutting direction of carbon fiber, [75, 194, 195], especially when the fibers are angled at −45° to the direction of the cutting speed [41, 196, 197]. However, excessive drilling temperature causes interfacial debonding of the carbon fiber and resin, which can lead to surface cracks, carbon fiber pull-out flaws, matrix resin degradation, and ultimately matrix resin cavities [90]. The protruding fibers and hooking of the fibers to the stylus tips may also result in inaccurate findings, or at least, greatly varying readings [75].

A clear value for accepting or rejecting decisions is provided by the average roughness parameters. The arithmetic average heights of peaks and valleys recorded within the sampling length, L, are known as the arithmetic average roughness, or Ra, as indicated in Eq. 4 [38].

$$R_a = \frac{1}{L}\int_0^L |y(x)|dx \tag{4}$$

4.3 Burr formation

It is difficult to drill metal panels because some of the metal may plastically deform and not be fully evacuated, leaving sharp and uneven contour around the hole that emerge above the surface of the work piece and induce stress concentrations that could lead to fatigue failures, corrosion, and a shorter lifespan for the aircraft [198]. Burr formations are the residual sharp edges, which typically appear on both sides of the drilled hole. The burr produced at the hole's entrance is usually smaller than the burr produced at the hole's exit. Additionally, by chamfering the hole, entry burrs can be removed easily [199], and if not handled

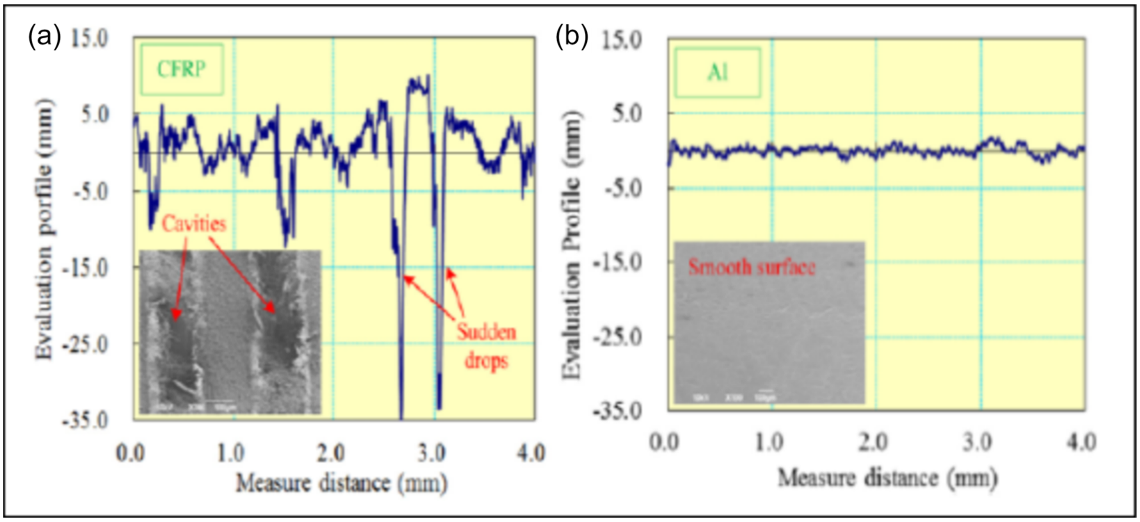

Fig. 24 Assessment contour and SEM photos of the hole surface under the drilling parameters of 2000 rpm and 0.06 mm/rev. **a** Ra = 2.664 µm for CFRP, **b** Ra = 0.488 µm for Al [90]

appropriately, the burrs generated at the exit of the hole are far more problematic to remove [199, 200]. Burr formation occurs in three stages: initiation, when plastic deformation starts; development, when deformation increases while cutting pressure falls; and formation, when only plastic deformation takes place and the burr takes on its final shape [201, 202]. The height, thickness, and radius can all be used to characterize the burr's shape [203]. Burr development near the hole's exit can cause deburring to require up to 40% of the entire machining time and raise overall expenses by 30% [204–207]. Burr thickness also has a larger influence on deburring costs, even if burr height is the most considered characteristic when it comes to burr measures [208]. The geometry of the tool and the drilling process's parameters have a major impact on the burr development [209].

Typically, there are three types of drilling-induced metallic part burrs: uniform type, transitory type, and crown type [201]. As shown in Fig. 25, while a crown burr usually has a severe roller-back or a crown shape that indicates the crack initially occurred at the cutting-edge drill point, a uniform burr type has a very modest uniform burr formation. Transient burr forms during the transitional stages between uniform burr and crown burr. Initial and secondary fractures occur virtually simultaneously at the center of the hole and on the periphery for transitory burr, which is caused by a degree of plastic deformation of metal near the end of the cutting edges that is almost similar to uniform burr [201].

The maximum burr formation value can be calculated using Eq. 5 [38].

$$H_{b_{max}} = measured_z - ref_z \quad (5)$$

where $H_{b\max}$ denotes maximum burr formation, *measured z* denotes measured location of the highest point, and *refz* denotes the surface panel of aluminum alloy.

A new concept known as "burr value" was established in order to more accurately characterize the burr as shown in Eq. 6. As depicted in Fig. 26, it includes the burr height (b_h), burr root thickness (b_r), burr thickness (b_t), and burr root radius (r_f). Burr height and thickness are the two-burr metrics that are used to calculate the burr [211]. Burr root thickness is the thickness of the burr root area as measured in

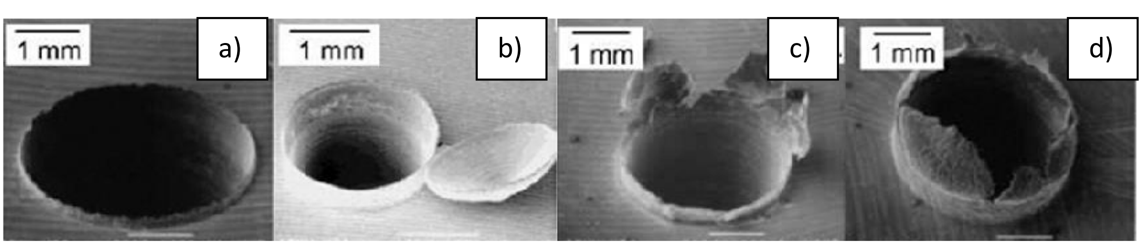

Fig. 25 Burr-type classification for drilling a stack material (**a**) uniform burr, (**b**) uniform burr with cap, (**c**) crown burr, and (**d**) transient burr [210]

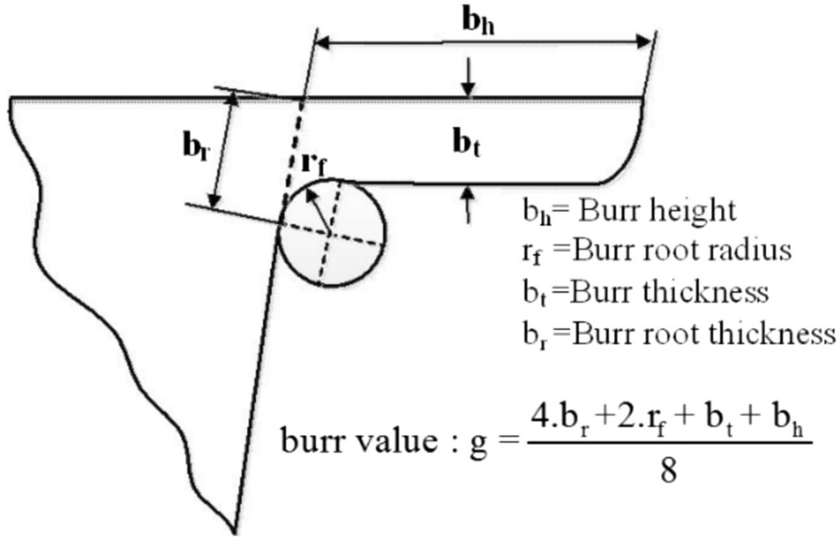

Fig. 26 Burr formation nomenclature [213]

the cross-section (b_r). The distance between the workpiece's ideal edge and the highest point in the cross-sectional area is known as the burr height (b_h). The burr root radius (r_f) is determined by positioning a circle to the burr root. As measured in the cross-section, the burr thickness (b_t) indicates the thickness parallel to the burr root area at a distance of r_f [212, 213].

$$Burrvalueg = \frac{4b_r + 2r_f + b_t + b_h}{8} \tag{6}$$

It should be noted that the drilling sequence (CFRP to aluminum or aluminum to CFRP) also has some effect in the burr formation. If it is from aluminum to CFRP drilling sequence, the exit burr height will be small compared to CFRP to aluminum drilling sequence. This difference is because of the supportive role of the bottom CFRP panel when drilling in the sequence of aluminum to CFRP, which increased the stiffness of the exit Al layer making it easier to shear the bottom surface layers and contributed to reduced exit Al burr defect. This support is absent when drilling from CFRP to aluminum side and therefore comparatively larger burr height may be obtained.

4.4 Delamination

Delamination damage is the most serious defect among all defects, accounting for around 60% of CFRP part rejections [214]. According to Sandvick Coromant tool manufacturers, the maximum allowable delamination is 1 mm [186]. When the thrust force of the drill exceeds the interlaminar fracture toughness of the layers, delamination occurs, which leads to decreased assembly tolerance and structural integrity [33]. Delamination means matrix melting or burning, formation of surface micro-cracks, and some pulled out fibers [215]. Both type of drilling-induced delamination such as peel up and push down can take place at the workpiece's entrance and exit planes, respectively [216]. Both these types of delamination mechanisms, as depicted in Fig. 27, are primarily driven by the thrust force created while drilling [23], and hence there is a critical thrust force value which delamination may be prevented below [170]. The upper layers of composite material in the peel-up delamination mechanism probably would be forced through the drill's cutting faces as it progresses rather than being sliced. According to Hocheng and Dharan's research, the cutting force operating at the periphery that generates a peeling force in the axial direction through the drill flute's slope is what causes peel-up delamination [182]. According to a few researchers, peel up delamination at the hole's entry becomes more serious than push out delamination at the hole's exit, in addition to being caused by metallic chip removal through the hole [48, 88, 132]. Conversely, push down delamination at the hole's exit becomes more serious than peel up delamination at the hole's entry because of the indentation effect working across the uncut layers of the laminate [23, 33]. The location of the damage is at the −45° angle formed by the direction of drill rotation with entangled chips and the fiber orientation. It is not entirely concentrated around the hole's entry. However, the most well-known method for reducing this particular delamination is to place a support plate underneath the work piece [125].

Different equations used by various researchers to quantify delamination are shown in Table 6. D_{nom} denotes the nominal hole diameter, D_{max} denotes the maximum delamination diameter, $F_{d\ min}$ denotes the minimum delamination factor, D_{min} denotes the minimum diameter of the hole, R_{max} denotes the radius of the maximum damage, and R denotes the drilled hole number in 1D delamination measurement. 2D delamination coefficient can more properly provide the

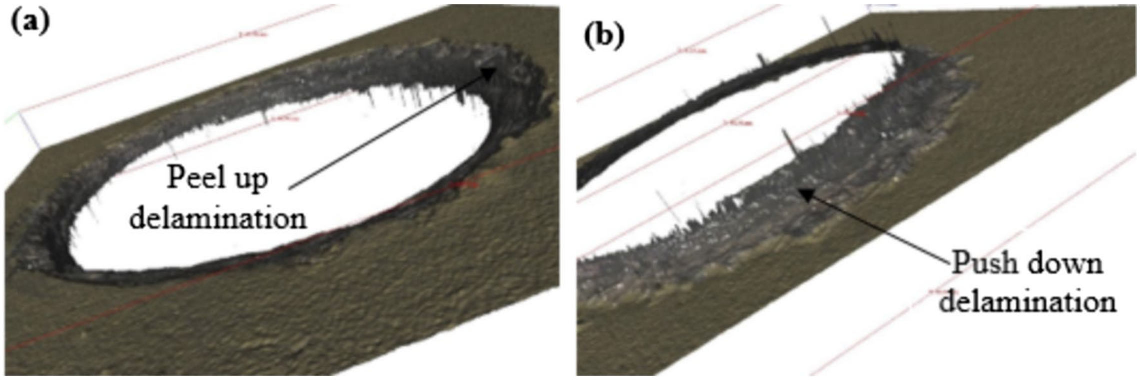

Fig. 27 **a** Peel up and **b** push down delamination [193]

size of the actual delamination zone and the evaluation criterion compared to the 1D delamination coefficient. In 2D delamination calculation, A_{nom} denotes the nominal hole area, A_{del} denotes the maximum delamination area, D_f is the delamination factor, and F_a is the 2D delamination factor. In comparison to the traditional 1D and 2D delamination factors, the 3D delamination factor presents a substantially higher precision for quantifying the delamination extents [170]. In the 3D delamination equations, A_d^k and A_{nom} stands for the delaminated area of the k^{th} CFRP layer and the nominal drilled hole area; p represents the total number of the delaminated layers and h denotes the thickness of one single CFRP layer.

5 Conclusion

In this paper, a review of process improvement and performance measurement of manufacturing defect in drilling CFRP/aluminum stack up panel has been presented according to the substantial previous works that are related to the current study.

- Achieving close tolerance in stack up diameter deviation, hole wall surface roughness, exit burrs height, and hole delamination is necessary to meet the aerospace industry standards of drilling CFRP/Al stack panel. Numerous researchers have shown that the drilling performances are significantly influenced by the cutting environment, the cutting tool, and the cutting parameters.
- In general, smaller drill geometric features, such as helix angle, point angle, and chisel edge length, generate better holes than larger ones. Twist drills perform better than double cone drills for drilling CFRP/Al stacks.
- Low feed rate and high cutting speed are typically the best parameters for CFRP/Al stacks drilling. Changing the cutting speed had little to no impact while changing the feed rate enhanced the cutting forces and torque.
- The use of nano coated drills is effective in reducing the cutting force, hole surface roughness, and improving the surface morphology compared to the uncoated drills. Among these coatings, diamond, tungsten, and DLC coating outperformed the rest. Due to their high cost, diamond-coated cutting tools are not frequently utilized; therefore, tungsten-coated carbide drills provide the best balance of price and cutting tool quality.
- Flood cooling, minimum quantity liquid (MQL) cooling, and cryogenic cooling can be executed to reduce hole damage. Liquid nitrogen and liquid carbon dioxide are highly used coolants. Rapid cooling, quick chip evacuation, prevention of chip accumulation, and enhanced chip breakage are some salient features which can be achieved through cooling.
- With MQL technique, friction is minimized and thereby cutting temperature decreases, tool life increases, and sur-

Table 6 Equations used by researchers to calculate delamination

Type of delamination	Equation	Reference
1D delamination	$F_{d=}\frac{D_{max}}{D_{nom}}$	[217]
	$F_{dmin=}\frac{D_{min}}{D_{nom}}$	[218]
	$Delaminationsize = R_{max} - R$	[33]
2D delamination	$D_{RAT} = \frac{A_{del}}{A_{nom}}$	[132, 219]
	$D_f = \left[\frac{A_{del}-A_{nom}}{A_{nom}}\right]100\%$	[132]
	$F_{a=}(\frac{A_{del}}{A_{nom}})\%$	[14]
	$F_{ad} = \alpha\frac{D_{max}}{D_{nom}} + \beta\frac{A_{del}}{A_{nom}}$ where $\alpha = 1 - \beta$ and $\beta = \frac{A_{del}}{A_{max}-A_{nom}}$	[214]
	$F_e = \frac{D_e}{D}$ where $D_e = \sqrt{4(A_{del} + A_{nom})/\pi}$	[220]
3D delamination	$F_v = V_d/V_{nom}$; where $V_d = \sum_{k=1}^{p} hA_d^k$; and $V_{nom} = p.h.A_{nom}$ $F_v = 1/p\sum_{k=1}^{p}\frac{A_d^k}{A_{nom}} = 1/p\sum_{k=1}^{p}F_a^k$	[221]

face quality improves significantly. With pressure, flow, and direction of MQL, the results may change accordingly.
- According to tool manufacturers, aircraft industries, and researchers, the maximum allowable diameter error is ± 30 μm, maximum accepted surface roughness for CFRP is 3.2 μm and for metal part is 1.6 μm, maximum allowable burr height is 100 μm, and maximum permissible delamination is 1 mm.
- The tables show that the hole circularity and hole cylindricity in stack up drilling are explored by very few researchers, which gives the impression that the priority of these parameters is less, but in reality, it is not the case. So substantial research on these parameters is necessary.
- Though there are many coatings developed and tried, the tribological characterization of these coatings have not been reported by any researchers so far under this application. Further analysis on bond strength, hardness, and coefficient of friction of coated drill bits may be needed to find a better coating.
- Combination of coating application, cooling strategy, better tool geometry, and optimum drilling parameters may be helpful in providing an optimum drilling environment to improve the hole quality and expand the tool life.

Author contribution Both authors contributed to the study conception and design. J. Joy Mathavan was involved in conceptualization, analysis, writing—original draft, formatting, and editing and M. H. Hassan was involved in conceptualization, supervision, fund acquisition, project administration, validation, and writing—review.

Funding The authors are grateful for the financial support provided by the Ministry of Higher Education Malaysia for Fundamental Research Grant Scheme with Project Code: FRGS/1/2022/TK10/USM/03/5. In addition, the authors greatly appreciate the School of Mechanical Engineering, USM's facility support.

Data Availability Data sharing not applicable to this article as no datasets were generated or analyzed during the current study.

Declarations

Competing interests The authors declare no competing interests..

References

1. Impero F, Dix M, Squillace A, Prisco U, Palumbo B, Tagliaferri F (2018) A comparison between wet and cryogenic drilling of CFRP/Ti stacks. Mater Manuf Processes 33(12):1354–1360. https://doi.org/10.1080/10426914.2018.1453162
2. Pawar OA, Gaikhe YS, Tewari A, Sundaram R, Joshi SS (2015) Analysis of hole quality in drilling GLARE fiber metal laminates. Compos Struct 123:350–365. https://doi.org/10.1016/J.COMPSTRUCT.2014.12.056
3. Geier N, Davim JP, Szalay T (2019) Advanced cutting tools and technologies for drilling carbon fibre reinforced polymer (CFRP) composites: a review. Compos Part A Appl Sci Manuf 125:105552. https://doi.org/10.1016/J.COMPOSITESA.2019.105552
4. Joy Mathavan J, Hassan MH, Xu J, Franz G (2022) Hole quality observation in single-shot drilling of CFRP/Al7075-T6 composite metal stacks using customized twist drill design. J Compos Sci 6(12):378. https://doi.org/10.3390/jcs6120378
5. Xu J, Zhou L, Chen M, Ren F (2019) Experimental study on mechanical drilling of carbon/epoxy composite-Ti6Al4V stacks. Mater Manuf Processes 34(7):715–725. https://doi.org/10.1080/10426914.2019.1594275
6. Li C, Xu J, Chen M, An Q, El Mansori M, Ren F (2019) Tool wear processes in low frequency vibration assisted drilling of CFRP/Ti6Al4V stacks with forced air-cooling. Wear 426–427:1616–1623. https://doi.org/10.1016/j.wear.2019.01.005
7. Xu J, El Mansori M, Voisin J, Chen M, Ren F (2019) On the interpretation of drilling CFRP/Ti6Al4V stacks using the orthogonal cutting method: chip removal mode and subsurface damage formation. J Manuf Process 44:435–447. https://doi.org/10.1016/j.jmapro.2019.05.052
8. Pramanik A, Littlefair G (2014) Developments in machining of stacked materials made of CFRP and titanium/aluminum alloys. Mach Sci Technol 18(4):485–508. https://doi.org/10.1080/10910344.2014.955718
9. Xu J, Mkaddem A, El Mansori M (2016) Recent advances in drilling hybrid FRP/Ti composite: a state-of-the-art review. Compos Struct 135:316–338. https://doi.org/10.1016/j.compstruct.2015.09.028
10. JWG Ad Vlot, Ed., Fibre metal laminates: an introduction., 1st ed. Springer Dordrecht, 2001. https://doi.org/10.1007/978-94-010-0995-9
11. Giasin K, Hawxwell J, Sinke J, Dhakal H, Köklü U, Brousseau E (2020) The effect of cutting tool coating on the form and dimensional errors of machined holes in GLARE® fibre metal laminates. Intl J Adv Manuf Technol 107(5):2817–2832. https://doi.org/10.1007/s00170-020-05211-2
12. Yapici A, Özkan V, Yıldız M, Erdal MO, Gemi L, Yazman Ş (2016) The effect of nylon 6.6 nanofiber layers on mechanical properties of epoxy. Int J Eng Sci (Ghaziabad) 5(11):86–89. https://doi.org/10.9790/1813-0511028689
13. Akif Doğan M, Yazman Ş, Gemi L, Yıldız M, Yapıcı A (2022) A review on drilling of FML stacks with conventional and unconventional processing methods under different conditions. Compos Struct. 297:115913. https://doi.org/10.1016/j.compstruct.2022.115913
14. Faraz A, Biermann D, Weinert K (2009) Cutting edge rounding: an innovative tool wear criterion in drilling CFRP composite laminates. Int J Mach Tools Manuf 49(15):1185–1196. https://doi.org/10.1016/J.IJMACHTOOLS.2009.08.002
15. Rawat S, Attia H (2009) Wear mechanisms and tool life management of WC–Co drills during dry high speed drilling of woven carbon fibre composites. Wear 267:1022–1030. https://doi.org/10.1016/j.wear.2009.01.031
16. Lin SC, Chen IK (1996) Drilling carbon fiber-reinforced composite material at high speed. Wear 194(1–2):156–162. https://doi.org/10.1016/0043-1648(95)06831-7
17. Chen WC (1997) Some experimental investigations in the drilling of carbon fiber-reinforced plastic (CFRP) composite laminates. Int J Mach Tools Manuf 37(8):1097–1108. https://doi.org/10.1016/S0890-6955(96)00095-8
18. Anand RS, Patra K (2017) Mechanistic cutting force modelling for micro-drilling of CFRP composite laminates. CIRP J

Manuf Sci Technol 16:55–63. https://doi.org/10.1016/J.CIRPJ.2016.07.002

19. Seeholzer L, Scheuner D, Wegener K (2020) Analytical force model for drilling out unidirectional carbon fibre reinforced polymers (CFRP). J Mater Process Technol 278:116489. https://doi.org/10.1016/j.jmatprotec.2019.116489
20. Zitoune R, Krishnaraj V, Collombet F, Le Roux S (2016) Experimental and numerical analysis on drilling of carbon fibre reinforced plastic and aluminium stacks. Compos Struct 146:148–158
21. König W, Wulf Ch, Graß P, Willerscheid H (1985) Machining of fibre reinforced plastics. CIRP Ann 34(2):537–548. https://doi.org/10.1016/S0007-8506(07)60186-3
22. Hocheng H, Tsao CC (2006) Effects of special drill bits on drilling-induced delamination of composite materials. Int J Mach Tools Manuf 46(12):1403–1416. https://doi.org/10.1016/j.ijmachtools.2005.10.004
23. Krishnaraj V et al (2012) Optimization of machining parameters at high speed drilling of carbon fiber reinforced plastic (CFRP) laminates. Compos B Eng 43(4):1791–1799. https://doi.org/10.1016/j.compositesb.2012.01.007
24. Park K-H, Beal A, Dae-W D, Kim P. Kwon, Lantrip J (2011) Tool wear in drilling of composite/titanium stacks using carbide and polycrystalline diamond tools. Wear 271(1–12):2826–2835. https://doi.org/10.1016/j.wear.2011.05.038
25. Ramulu M, Branson T, Kim D (2001) A study on the drilling of composite and titanium stacks. Compos Struct 54(1):67–77. https://doi.org/10.1016/S0263-8223(01)00071-X
26. Wang X, Kwon PY, Sturtevant C, Kim DDW, Lantrip J (2014) Comparative tool wear study based on drilling experiments on CFRp/Ti stack and its individual layers. Wear 317(1–2):265–276. https://doi.org/10.1016/j.wear.2014.05.007
27. Denkena B, Boehnke D, Dege JH (2008) Helical milling of CFRP–titanium layer compounds. CIRP J Manuf Sci Technol 1(2):64–69. https://doi.org/10.1016/j.cirpj.2008.09.009
28. Altin Karataş M, Gökkaya H (2018) A review on machinability of carbon fiber reinforced polymer (CFRP) and glass fiber reinforced polymer (GFRP) composite materials. Defence Technol 14(4):318–326. https://doi.org/10.1016/J.DT.2018.02.001
29. Aamir M, Tolouei-Rad M, Giasin K, Nosrati A (2019) Recent advances in drilling of carbon fiber–reinforced polymers for aerospace applications: a review. Intl J Adv Manuf Technol 105(5):2289–2308. https://doi.org/10.1007/s00170-019-04348-z
30. Giasin K, Ayvar-Soberanis S (2017) An investigation of burrs, chip formation, hole size, circularity and delamination during drilling operation of GLARE using ANOVA. Compos Struct 159:745–760. https://doi.org/10.1016/j.compstruct.2016.10.015
31. Giasin K (2016) Machining fibre metal laminates and Al2024-T3 aluminium alloy. PhD thesi, p 309
32. Giasin K (2018) The effect of drilling parameters, cooling technology, and fiber orientation on hole perpendicularity error in fiber metal laminates. Int J Adv Manuf Technol 97(9–12):4081–4099. https://doi.org/10.1007/s00170-018-2241-1
33. El-Sonbaty I, Khashaba UA, Machaly T (2004) Factors affecting the machinability of GFR/epoxy composites. Compos Struct 63(3):329–338. https://doi.org/10.1016/S0263-8223(03)00181-8
34. Abrão AM, Rubio JCC, Faria PE, Davim JP (2008) The effect of cutting tool geometry on thrust force and delamination when drilling glass fibre reinforced plastic composite. Mater Des 29(2):508–513. https://doi.org/10.1016/J.MATDES.2007.01.016
35. Giasin K, Ayvar-Soberanis S, French T, Phadnis V (2017) 3D finite element modelling of cutting forces in drilling fibre metal laminates and experimental hole quality analysis. Appl Compos Mater 24(1):113–137. https://doi.org/10.1007/s10443-016-9517-0
36. Giasin K, Hodzic A, Phadnis V, Ayvar-Soberanis S (2016) Assessment of cutting forces and hole quality in drilling Al2024 aluminium alloy: experimental and finite element study. Int J Adv Manuf Technol 87(5–8):2041–2061. https://doi.org/10.1007/s00170-016-8563-y
37. Zitoune R, Krishnaraj V, Collombet F (2010) Study of drilling of composite material and aluminium stack. Compos Struct 92(5):1246–1255. https://doi.org/10.1016/J.COMPSTRUCT.2009.10.010
38. Hassan MH (2020) Optimization of customized twist drill geometry for single-shot drilling of composite-metal stack. PhD thesi, pp 1–191
39. Soo SL, Abdelhafeez AM, Li M, Hood R, Lim CM (2019) The drilling of carbon fibre composite–aluminium stacks and its effect on hole quality and integrity. Proc Inst Mech Eng B J Eng Manuf 233(4):1323–1331. https://doi.org/10.1177/0954405417728312
40. Mahdi A, Turki Y, Habak M, Salem M, Bouaziz Z (2020) Experimental study of thrust force and surface quality when drilling hybrid stacks. The Int J Adv Manuf Technol 107(9):3981–3994. https://doi.org/10.1007/s00170-020-05252-7
41. Zitoune R, Collombet F, Lachaud F, Piquet RD, Pasquet P (2005) Experiment–calculation comparison of the cutting conditions representative of the long fiber composite drilling phase. Compos Sci Technol 65:455–466
42. Bhatnagar N, Nayak D, Singh I, Chouhan H, Mahajan P (2004) Determination of machining-induced damage characteristics of fiber reinforced plastic composite laminates. Mater Manuf Processes 19(6):1009–1023. https://doi.org/10.1081/AMP-200035177
43. Rodríguez A, Calleja A, de Lacalle LNL, Pereira O, Rubio-Mateos A, Rodríguez G (2021) Drilling of CFRP-Ti6Al4V stacks using CO2-cryogenic cooling. J Manuf Process 64(2020):58–66. https://doi.org/10.1016/j.jmapro.2021.01.018
44. Zitoune R, El Mansori M, Krishnaraj V (2013) Tribo-functional design of double cone drill implications in tool wear during drilling of copper mesh/CFRP/woven ply. Wear 302(1):1560–1567. https://doi.org/10.1016/j.wear.2013.01.046
45. Zitoune R, Krishnaraj V, Sofiane Almabouacif F, Belkacem Collombet, Sima M, Jolin A (2012) Influence of machining parameters and new nano-coated tool on drilling performance of CFRP/Aluminium sandwich. Compos B Eng 4(3):1480–1488. https://doi.org/10.1016/j.compositesb.2011.08.054
46. Shyha IS et al (2011) Hole quality assessment following drilling of metallic-composite stacks. Int J Mach Tools Manuf 51(7–8):569–578. https://doi.org/10.1016/j.ijmachtools.2011.04.007
47. Kim D, Ramulu M (2004) Drilling process optimization for graphite/bismaleimide–titanium alloy stacks. Compos Struct 63(1):101–114. https://doi.org/10.1016/S0263-8223(03)00137-5
48. Brinksmeier E, Janssen R (2002) Drilling of multi-layer composite materials consisting of carbon fiber reinforced plastics (CFRP), titanium and aluminum alloys. CIRP Ann 51(1):87–90. https://doi.org/10.1016/S0007-8506(07)61472-3
49. Hocheng H, Puw HY (1992) On drilling characteristics of fiber-reinforced thermoset and thermoplastics. Int J Mach Tools Manuf 32(4):583–592. https://doi.org/10.1016/0890-6955(92)90047-K
50. Davim JP, Reis P, António CC (2004) Experimental study of drilling glass fiber reinforced plastics (GFRP) manufactured by hand lay-up. Compos Sci Technol 64(2):289–297. https://doi.org/10.1016/S0266-3538(03)00253-7
51. Sinmazçelik T, Avcu E, Bora MÖ, Çoban O (2011) A review: fibre metal laminates, background, bonding types and applied test methods. Mater Des 32(7):3671–3685. https://doi.org/10.1016/j.matdes.2011.03.011
52. Qaiser H, Umar S, Nasir A, Shah M, Nauman S (2015) Optimization of interlaminar shear strength behavior of anodized and unanodized ARALL composites fabricated through VARTM process. IntJ Mater Form 8(3):481–493. https://doi.org/10.1007/s12289-014-1192-9

53. Freischmidt G, Coutts RSP, Janardhana MN (1994) Aluminium/lithium alloy-carbon fibre/epoxy laminated hybrid composite material Part I Preliminary results. J Mater Sci Lett 13(14):1027–1031. https://doi.org/10.1007/BF00277029
54. Giasin K, Ayvar-Soberanis S, Hodzic A (2016) Evaluation of cryogenic cooling and minimum quantity lubrication effects on machining GLARE laminates using design of experiments. J Clean Prod 135:533–548. https://doi.org/10.1016/j.jclepro.2016.06.098
55. Giasin K, Ayvar-Soberanis S, Hodzic A (2015) An experimental study on drilling of unidirectional GLARE fibre metal laminates. Compos Struct 133:794–808. https://doi.org/10.1016/j.compstruct.2015.08.007
56. K Giasin and S Ayvar-Soberanis (2016) "Evaluation of workpiece temperature during drilling of GLARE fiber metal laminates using infrared techniques: effect of cutting parameters, fiber orientation and spray mist application," Materials 9(8) https://doi.org/10.3390/ma9080622.
57. Patel D, Verma R (2015) Analysis of drilling tool life — a review. Int J Mech Eng Rob Res 4(1):685–691
58. Starke EA, Staley JT (1996) Application of modern aluminum alloys to aircraft. Prog Aerosp Sci 32(2):131–172. https://doi.org/10.1016/0376-0421(95)00004-6
59. Mouritz AP (2012) Introduction to aerospace materials. Woodhead Publishing Limited
60. Santos MC, Machado AR, Sales WF, Barrozo MAS, Ezugwu EO (2016) Machining of aluminum alloys: a review. Int J Adv Manuf Technol 86(9):3067–3080. https://doi.org/10.1007/s00170-016-8431-9
61. Campbell FC (2008) Aluminium. In: Elements of metallurgy and engineering alloys, ASM International, pp 487–508. https://doi.org/10.31399/asm.tb.emea.t52240487
62. Verma BB, Atkinson JD, Kumar M (2001) Study of fatigue behaviour of 7475 aluminium alloy. Bull Mater Sci 24(2):231–236. https://doi.org/10.1007/BF02710107
63. Williams JC, Starke EA (2003) Progress in structural materials for aerospace systems. Acta Mater 51:5775–5799
64. Dursun T, Soutis C (2014) Recent developments in advanced aircraft aluminium alloys. Mater Des 1980–2015(56):862–871. https://doi.org/10.1016/j.matdes.2013.12.002
65. Zhang L, Liu Z, Tian W, Liao W (2015) Experimental studies on the performance of different structure tools in drilling CFRP/Al alloy stacks. Int J Adv Manuf Technol 81(1):241–251. https://doi.org/10.1007/s00170-015-6955-z
66. Cheng H, Zhang K, Wang N, Luo B, Meng Q (2017) A novel six-state cutting force model for drilling-countersinking machining process of CFRP-Al stacks. Int J Adv Manuf Technol 89(5–8):2063–2076. https://doi.org/10.1007/s00170-016-9236-6
67. R Garrick (2007) "Drilling of advanced aircraft structure with poly-crystalline diamond (PCD) drills." Aerospace technology conference and exposition Los Angels, California United states https://doi.org/10.4271/2007-01-3893
68. Xu J, El Mansori M, Chen M, Ren F (2019) Orthogonal cutting mechanisms of CFRP/Ti6Al4V stacks. Int J Adv Manuf Technol 103(9):3831–3851. https://doi.org/10.1007/s00170-019-03734-x
69. An Q, Dang J, Li J, Wang C, Chen M (2020) Investigation on the cutting responses of CFRP/Ti stacks: with special emphasis on the effects of drilling sequences. Compos Struct 253:112794. https://doi.org/10.1016/j.compstruct.2020.112794
70. Karpat Y, Bahtiyar O, Değer B, Kaftanoğlu B (2014) A mechanistic approach to investigate drilling of UD-CFRP laminates with PCD drills. CIRP Ann Manuf Technol 63(1):81–84. https://doi.org/10.1016/j.cirp.2014.03.077
71. Kim D, Ramulu M (2007) Study on the drilling of titanium/graphite hybrid composites. J Eng Mater Technol 129(3):390–396. https://doi.org/10.1115/1.2744397
72. Hocheng H (2012) Machining technology for composite materials: principles and practice. Woodhead Publishing Limited
73. Vijayan K, Zitoune R, Collombet F (2010) Comprehensive review on drilling of multimaterials stacks. J Mach Form Technol 2(3/4):171–200
74. Komanduri R (1997) Machining of fiber-reinforced composites. Mach Sci Technol 1(1):113–152. https://doi.org/10.1080/10940349708945641
75. König W, Graß P (1989) Quality definition and assessment in drilling of fibre reinforced thermosets. CIRP Ann 38(1):119–124. https://doi.org/10.1016/S0007-8506(07)62665-1
76. Oberg E, Jones FD, Horton HL, Ryffel HH (2004) Machinery's Handbook (27th edn) & Guide to Machinery's Handbook. New York
77. Khan ZM (1991) A study of the drilling of advanced carbon fibre composites. University of Salford Manchester, PhD
78. Heisel U, Pfeifroth T (2012) Influence of point angle on drill hole quality and machining forces when drilling CFRP. Procedia CIRP 1(1):471–476. https://doi.org/10.1016/j.procir.2012.04.084
79. Gaitonde VN, Karnik SR, Achyutha BT, Siddeswarappa B (2007) Methodology of Taguchi optimization for multi-objective drilling problem to minimize burr size. Int J Adv Manuf Technol 34(1):1–8. https://doi.org/10.1007/s00170-006-0571-x
80. Hassan MH, Abdullah J, Franz G, Shen CY, Mahmoodian R (2021) Effect of twist drill geometry and drilling parameters on hole quality in single-shot drilling of CFRP / Al7075-T6 composite stack. J Compos Sci 5:189
81. Hassan MH, Jamaluddin A, Franz G (2022) Multi-objective optimization in single-shot drilling of CFRP/Al stacks using customized twist drill. Materials 15(5):279–286. https://doi.org/10.3390/ma15051981
82. Wei Y, An Q, Ming W, Chen M (2016) Effect of drilling parameters and tool geometry on drilling performance in drilling carbon fiber-reinforced plastic/titanium alloy stacks. Adv Mech Eng 8(9):1–16. https://doi.org/10.1177/1687814016670281
83. Loja MAR, Alves MSF, Bragança IMF, Rosa RSB, Barbosa ICJ, Barbosa JI (2018) An assessment of thermally influenced and delamination-induced regions by composites drilling. Compos Struct 202:413–423. https://doi.org/10.1016/j.compstruct.2018.02.046
84. Feito N, Diaz-Alvarez J, Lopez-Puente J, Miguelez MH (2018) Experimental and numerical analysis of step drill bit performance when drilling woven CFRPs. Compos Struct 184:1147–1155. https://doi.org/10.1016/j.compstruct.2017.10.061
85. Piquet R, Ferret B, Lachaud F, Swider P (2000) Experimental analysis of drilling damage in thin carbon/epoxy plate using special drills. Compos Part A Appl Sci Manuf 31(10):1107–1115. https://doi.org/10.1016/S1359-835X(00)00069-5
86. Neugebauer R, Ben-Hanan U, Ihlenfeldt S, Wabner M, Stoll A (2012) Acoustic emission as a tool for identifying drill position in fiber-reinforced plastic and aluminum stacks. Int J Mach Tools Manuf 57:20–26. https://doi.org/10.1016/j.ijmachtools.2012.01.013
87. Wertheim R, Ben-Hanan U, Ihlenfeldt S, Stoll A, Treppe F, Wabner M (2012) Acoustic emission for controlling drill position in fiber-reinforced plastic and metal stacks. CIRP Ann 61(1):75–78. https://doi.org/10.1016/j.cirp.2012.03.003
88. Montoya M, Calamaz M, Gehin D, Girot F (2013) Evaluation of the performance of coated and uncoated carbide tools in drilling thick CFRP/aluminium alloy stacks. Int J Adv Manuf Technol 68(9):2111–2120. https://doi.org/10.1007/s00170-013-4817-0
89. Zitoune R, Cadorin N, Elambouacif BS, Collombet F, Krishnaraj V, Bougherara H (2014) Influence of the double cone drill geometry on the holes quality during drilling multi-stack made of CFRP/Al. Int J Mater Mech Manuf 2(4):292–296. https://doi.org/10.7763/ijmmm.2014.v2.145
90. Wang C-Y, Chen Y-H, An Q-L, Cai X-J, Ming W-W, Chen M (2015) Drilling temperature and hole quality in drilling of

CFRP/aluminum stacks using diamond coated drill. Int J Precis Eng Manuf 16(8):1689–1697. https://doi.org/10.1007/s12541-015-0222-y
91. Kuo CL et al (2018) Development of single step drilling technology for multilayer metallic-composite stacks using uncoated and PVD coated carbide tools. J Manuf Process 31:286–300. https://doi.org/10.1016/j.jmapro.2017.11.026
92. Xu J, An Q, Cai X, Chen M (2013) Drilling machinability evaluation on new developed high-strength T800S/250F CFRP laminates. Int J Precis Eng Manuf 14(10):1687–1696. https://doi.org/10.1007/s12541-013-0252-2
93. C Ramírez Alcalá, F Torres Pineda, and M Horn, (2014) "CFRP and aluminum stacks drilled in one drilling step in 25 microns of tolerance," 16th Euro Conf Compos Mater ECCM 2014 22–26.
94. An M, Xu QL, Cai JY, Chen XJ (2013) Experimental investigation on drilling force and hole quality when drilling of T800S/250F CFRP laminate. Adv Mater Res Trans Tech Publications Ltd 797:155–160. https://doi.org/10.4028/www.scientific.net/amr.797.155
95. An Q, Cai X, Xu J, Chen M (2014) Experimental investigation on drilling of high strength T800S/250F CFRP with twist and dagger drill bits. Int J Abras Technol 6(3):183–196. https://doi.org/10.1504/IJAT.2014.060690
96. Feito N, Muñoz-Sánchez A, Díaz-Álvarez A, Miguelez MH (2019) Multi-objective optimization analysis of cutting parameters when drilling composite materials with special geometry drills. Compos Struct 225:111187. https://doi.org/10.1016/j.compstruct.2019.111187
97. Kuo C et al (2014) Tool wear and hole quality when single-shot drilling of metallic-composite stacks with diamond-coated tools. Proc Inst Mech Eng B J Eng Manuf 228(10):1314–1322. https://doi.org/10.1177/0954405413517388
98. Batzer SA, Haan DM, Rao PD, Olson WW, Sutherland JW (1998) Chip morphology and hole surface texture in the drilling of cast Aluminum alloys. J Mater Process Technol 79(1–3):72–78. https://doi.org/10.1016/S0924-0136(97)00324-5
99. Rawat S, Attia H (2009) Characterization of the dry high speed drilling process of woven composites using Machinability Maps approach. CIRP Ann 58(1):105–108. https://doi.org/10.1016/j.cirp.2009.03.100
100. Geier N, Xu J, Pereszlai C, Poór DI, Davim JP (2020) Drilling of carbon fibre reinforced polymer (CFRP) composites: difficulties, challenges and expectations. Procedia Manuf 54:284–289. https://doi.org/10.1016/j.promfg.2021.07.045
101. Nouari M, List G, Girot F, Géhin D (2005) Effect of machining parameters and coating on wear mechanisms in dry drilling of aluminium alloys. Int J Mach Tools Manuf 45(12–13):1436–1442. https://doi.org/10.1016/j.ijmachtools.2005.01.026
102. Grzesik W (2000) The influence of thin hard coatings on frictional behaviour in the orthogonal cutting process. Tribol Int 33(2):131–140. https://doi.org/10.1016/S0301-679X(00)00072-4
103. Kim D, Ramulu M, Pedersen W (2005) Machinability of titanium/graphite hybrid composites in drilling. Trans North Am Manuf Res Instit SME 33:445–452
104. Kumar MS, Prabukarthi A, Krishnaraj V (2013) Study on tool wear and chip formation during drilling carbon fiber reinforced polymer (CFRP)/titanium alloy (Ti6Al4V) stacks. Procedia Eng 64:582–592. https://doi.org/10.1016/j.proeng.2013.09.133
105. Liu DF, Tang YJ, Cong WL (2012) A review of mechanical drilling for composite laminates. Compos Struct 94(4):1265–1279. https://doi.org/10.1016/J.COMPSTRUCT.2011.11.024
106. Kurt M, Kaynak Y, Bagci E (2008) Evaluation of drilled hole quality in Al 2024 alloy. Int J Adv Manuf Technol 37(11):1051–1060. https://doi.org/10.1007/s00170-007-1049-1
107. Rawat S, Attia H (2009) Characterization of the dry high speed drilling process of woven composites using Machinability Maps approach. CIRP Ann 58(1):105–108. https://doi.org/10.1016/J.CIRP.2009.03.100
108. Won MS, Dharan CKH (2002) Chisel edge and pilot hole effects in drilling composite laminates. J Manuf Sci Eng 124(2):242–247. https://doi.org/10.1115/1.1448317
109. Kuo CL et al (2014) The effect of cutting speed and feed rate on hole surface integrity in single-shot drilling of metallic-composite stacks. Procedia CIRP 13:405–410. https://doi.org/10.1016/j.procir.2014.04.069
110. Angelone R, Caggiano A, Improta I, Nele L, Teti R (2020) Roughness of composite materials: characterization of hole quality in drilling of Al/CFRP stacks. Procedia CIRP 88:473–478. https://doi.org/10.1016/j.procir.2020.05.082
111. Benezech L, Landon Y, Rubio W (2012) Study of manufacturing defects and tool geometry optimisation for multi-material stack drilling. Adv Mat Res 423:1–11. https://doi.org/10.4028/www.scientific.net/AMR.423.1
112. Graham T. Smith, (2002) Industrial metrology: surfaces and roundness, 1st ed. Springer London, https://doi.org/10.1007/978-1-4471-3814-3.
113. Gaitonde VN, Karnik SR, Achyutha BT, Siddeswarappa B (2008) Taguchi optimization in drilling of AISI 316L stainless steel to minimize burr size using multi-performance objective based on membership function. J Mater Process Technol 202(1):374–379. https://doi.org/10.1016/j.jmatprotec.2007.08.013
114. Rivero A, Aramendi G, Herranz S, Lacalle D, López LN (2006) An experimental investigation of the effect of coatings and cutting parameters on the dry drilling performance of aluminium alloys. Int J Adv Manuf Technol 28(1–2):1–11. https://doi.org/10.1007/s00170-004-2349-3
115. Kelly JF, Cotterell MG (2002) Minimal lubrication machining of aluminium alloys. J Mater Proc Tech 120(1–3):327–334
116. Hassan MH, Abdullah J, Mahmud AS, Supran A (2017) Burr height as quality indicator in single shot drilling of stacked CFRP/aluminium composite. Eng Mater Trans Tech Publications Ltd 744:327–331
117. Rajakumar IPT, Hariharan P, Srikanth I (2012) A study on monitoring the drilling of polymeric nanocomposite laminates using acoustic emission. J Compos Mater 47(14):1773–1784. https://doi.org/10.1177/0021998312451299
118. Paulo Davim J, Reis P, Conceição António C (2004) Drilling fiber reinforced plastics (FRPs) manufactured by hand lay-up: influence of matrix (Viapal VUP 9731 and ATLAC 382–05). J Mater Process Technol 155–156:1828–1833. https://doi.org/10.1016/j.jmatprotec.2004.04.173
119. Abrão AM, Faria PE, Rubio JCC, Reis P, Davim JP (2007) Drilling of fiber reinforced plastics: a review. J Mater Process Technol 186(1–3):1–7. https://doi.org/10.1016/j.jmatprotec.2006.11.146
120. Davim JP, Reis P (2003) Drilling carbon fiber reinforced plastics manufactured by autoclave-experimental and statistical study. Mater Des 24(5):315–324. https://doi.org/10.1016/S0261-3069(03)00062-1
121. Palanikumar K (2011) Experimental investigation and optimisation in drilling of GFRP composites. Measurement 44(10):2138–2148. https://doi.org/10.1016/j.measurement.2011.07.023
122. Davim JP, Reis P (2003) Study of delamination in drilling carbon fiber reinforced plastics (CFRP) using design experiments. Compos Struct 59(4):481–487
123. Tsao CC (2008) Investigation into the effects of drilling parameters on delamination by various step-core drills. J Mater Process Technol 206(1):405–411. https://doi.org/10.1016/j.jmatprotec.2007.12.057
124. Quan Y, Zhong W (2009) Investigation on drilling-grinding of CFRP. Front Mech Eng China 4(1):60–63. https://doi.org/10.1007/s11465-009-0008-y
125. Shyha IS, Aspinwall DK, Soo SL, Bradley S (2009) Drill geometry and operating effects when cutting small diameter

holes in CFRP. Int J Mach Tools Manuf 49(12):1008–1014. https://doi.org/10.1016/j.ijmachtools.2009.05.009
126. Marques AT, Durão LM, Magalhães AG, Silva JF, Tavares JMRS (2009) Delamination analysis of carbon fibre reinforced laminates: Evaluation of a special step drill. Compos Sci Technol 69(14):2376–2382. https://doi.org/10.1016/j.compscitech.2009.01.025
127. Gaitonde VN, Karnik SR, Rubio JC, Correia AE, Abrão AM, Davim JP (2008) Analysis of parametric influence on delamination in high-speed drilling of carbon fiber reinforced plastic composites. J Mater Process Technol 203(1):431–438. https://doi.org/10.1016/j.jmatprotec.2007.10.050
128. Grilo TJ, Paulo RMF, Silva CRM, Davim JP (2013) Experimental delamination analyses of CFRPs using different drill geometries. Compos B Eng 45(1):1344–1350. https://doi.org/10.1016/j.compositesb.2012.07.057
129. Durão LMP, Gonçalves DJS, Tavares JMRS, de Albuquerque VHC, Aguiar Vieira A, Torres Marques A (2010) Drilling tool geometry evaluation for reinforced composite laminates. Compos Struct 92(7):1545–1550. https://doi.org/10.1016/j.compstruct.2009.10.035
130. Campos Rubio JC, Abrão AM, Eustáquio Faria P, Correia AE, Davim JP (2008) Delamination in high-speed drilling of carbon fiber reinforced plastic (CFRP). J Compos Mater 42(15):1523–1532. https://doi.org/10.1177/0021998308092205
131. Ashrafi SA, Sharif S, Farid AA, Yahya MY (2013) Performance evaluation of carbide tools in drilling CFRP-Al stacks. J Compos Mater 48(17):1–14. https://doi.org/10.1177/0021998313494429
132. D'Orazio A, El Mehtedi M, Forcellese A, Nardinocchi A, Simoncini M (2017) Tool wear and hole quality in drilling of CFRP/AA7075 stacks with DLC and nanocomposite TiAlN coated tools. J Manuf Process 30:582–592. https://doi.org/10.1016/j.jmapro.2017.10.019
133. Wang G-D, Melly SK, Li N (2018) Experimental studies on a two-step technique to reduce delamination damage during milling of large diameter holes in CFRP/Al stack. Compos Struct 188:330–339. https://doi.org/10.1016/j.compstruct.2018.01.039
134. SR Fernandez-Vidal, S Fernandez-Vidal, M Batista, Salguero S (2018) "Tool wear mechanism in cutting of stack CFRP/UNS A97075," Materials (Basel) 11(8) https://doi.org/10.3390/ma11081276.
135. F. Bañon, S. Alejandro, S. Fernandez-Vidal, and S. R. Fernandez-Vidal, "One-Shot Drilling analysis of stack CFRP/UNS A92024 bonding by adhesive.," Materials (Basel), vol. 12, no. 1, Jan. 2019, https://doi.org/10.3390/ma12010160.
136. RHN Reddy, M Alphonse, VKB Raja, K Palanikumar, DRSK Sanjay, KVM Sudhan (2020) "Evaluating the wear studies and tool characteristics of coated and uncoated HSS drill bit - a review," Mater Today Proc (46)3779–3785 https://doi.org/10.1016/j.matpr.2021.02.022
137. Prajapati JP, Bhatt PM, Patel NS (2015) 'Force and wear analysis of PVD coated cutting tool' - a review. Int J Adv Res Innov Ideas Educ 1:9–16
138. Mathavan JJ, Patnaik A (2016) Analysis of wear properties of aluminium based journal bearing alloys with and without lubrication. IOP Conf Ser Mater Sci Eng 149:12052. https://doi.org/10.1088/1757-899x/149/1/012052
139. Brinksmeier E, Fangmann S, Rentsch R (2011) Drilling of composites and resulting surface integrity. CIRP Ann Manuf Technol 60(1):57–60. https://doi.org/10.1016/j.cirp.2011.03.077
140. VP Astakhov and JP Davim, (2008) "Tools (geometry and material) and tool wear BT - machining: fundamentals and recent advances," J P Davim, Ed., London: Springer London, pp. 29–57. https://doi.org/10.1007/978-1-84800-213-5_2
141. Karpat Y, Bahtiyar O (2015) Comparative analysis of PCD drill designs during drilling of CFRP laminates. Procedia CIRP 31:316–321. https://doi.org/10.1016/j.procir.2015.03.094
142. D Kim, A Beal, and P Kwon, (2015) "Effect of tool wear on hole quality in drilling of carbon fiber reinforced plastic–titanium alloy stacks using tungsten carbide and polycrystalline diamond tools," J Manuf Sci Eng 138(3) https://doi.org/10.1115/1.4031052.
143. Ferreira JR, Coppini NL, Miranda GWA (1999) Machining optimisation in carbon fibre reinforced composite materials. J Mater Process Technol 92–93:135–140. https://doi.org/10.1016/S0924-0136(99)00221-6
144. Park K-H, Kwon P, Dae-W Kim D (2012) Wear characteristic on BAM coated carbide tool in drilling of composite/titanium stack. Int J Precis Eng Manuf 13(7):1073–1076. https://doi.org/10.1007/s12541-012-0140-1
145. D Nguyen, V Voznyuk, MS Bin Abdullah, D. Kim, and P. Y. Kwon, (2019) "Tool wear of superhard ceramic coated tools in drilling of CFRP/Ti stacks," in International Manufacturing Science and Engineering Conferenc https://doi.org/10.1115/MSEC2019-2843
146. S Swan, MS Bin Abdullah, D Kim, D Nguyen, and P Kwon (2018) "Tool wear of advanced coated tools in drilling of CFRP," J Manuf Sci Eng 140(11) https://doi.org/10.1115/1.4040916
147. Wang X, Kwon PY, Sturtevant C, Dae-W Kim D, Lantrip J (2013) Tool wear of coated drills in drilling CFRP. J Manuf Process 15(1):127–135. https://doi.org/10.1016/j.jmapro.2012.09.019
148. Kuo C, Wang C, Ko S (2018) Wear behaviour of CVD diamond-coated tools in the drilling of woven CFRP composites. Wear 398–399:1–12. https://doi.org/10.1016/j.wear.2017.11.015
149. Che D, Saxena I, Han P, Guo P, Ehmann KF (2014) Machining of carbon fiber reinforced plastics/polymers: a literature review. J Manuf Sci Eng 136(3):034001. https://doi.org/10.1115/1.4026526
150. Heath PJ (2001) Developments in applications of PCD tooling. J Mater Process Technol 116(1):31–38. https://doi.org/10.1016/S0924-0136(01)00837-8
151. Butler-Smith PW et al (2015) A study of an improved cutting mechanism of composite materials using novel design of diamond micro-core drills. Int J Mach Tools Manuf 88:175–183. https://doi.org/10.1016/j.ijmachtools.2014.10.002
152. G Basmaci, AS Yoruk, U Koklu, S Morkavuk, (2017) "Impact of cryogenic condition and drill diameter on drilling performance of CFRP," Appl Sci (Switzerland) 7(7) https://doi.org/10.3390/app7070667
153. Zhao F, Clarens A, Murphree A, Hayes K, Skerlos SJ (2006) Structural aspects of surfactant selection for the design of vegetable oil semi-synthetic metalworking fluids. Environ Sci Technol 40(24):7930–7937. https://doi.org/10.1021/es061418l
154. Iskandar Y, Damir A, Attia MH, Hendrick P (2013) "On the effect of MQL parameters on machining quality of CFRP", in *ICCM International Conferences on Composite Materials*. Mechanical Engineering Department, McGill University, Montreal, Canada, International Committee on Composite Materials, pp 3281–3290
155. Meshreki M, Damir A, Sadek A, Attia MH (2016) Investigation of drilling of CFRP-aluminum stacks under different cooling modes. In: ASME 2016 International Mechanical Engineering Congress and Exposition. https://doi.org/10.1115/imece2016-67039
156. Iqbal A et al (2021) CFRP drilling under throttle and evaporative cryogenic cooling and micro-lubrication. Compos Struct 267:113916. https://doi.org/10.1016/j.compstruct.2021.113916
157. Seeholzer L, Spahni M, Wegener K (2021) Influence of different cooling strategies on the process temperatures and chip

transport quality in one-shot drilling CFRP/Al-stacks. Procedia CIRP 101:310–313. https://doi.org/10.1016/j.procir.2020.12.005
158. Janakiraman A, Pemmasani S, Sheth S, Kannan C, Balan ASS (2020) Experimental investigation and parametric optimization on hole quality assessment during drilling of CFRP/GFRP/Al stacks. J Instit Eng (India) Series C 101(2)291–302. https://doi.org/10.1007/s40032-020-00563-w
159. Abish J, Samal P, Narenther MS, Kannan C, Balan ASS (2018) Assessment of drilling-induced damage in CFRP under chilled air environment. Mater Manuf Processes 33(12):1361–1368. https://doi.org/10.1080/10426914.2017.1415452
160. Xia T, Kaynak Y, Arvin C, Jawahir IS (2016) Cryogenic cooling-induced process performance and surface integrity in drilling CFRP composite material. Int J Adv Manuf Technol 82(1):605–616. https://doi.org/10.1007/s00170-015-7284-y
161. Schutz JB (1998) Properties of composite materials for cryogenic applications. Cryogenics (Guildf) 38(1):3–12. https://doi.org/10.1016/S0011-2275(97)00102-1
162. Bertolini R, Alagan NT, Gustafsson A, Savio E, Ghiotti A, Bruschi S (2022) Ultrasonic vibration and cryogenic assisted drilling of aluminum-CFRP composite stack – an innovative approach. Procedia CIRP 108:94–99. https://doi.org/10.1016/j.procir.2022.03.020
163. F Kneubühler, L Seeholzer, M Spahnia, L Di Piernoa, K Wegener, (2021) "Method for evaluating cooling strategies in terms of chip formation/transport in drilling CFRP/Al-stacks-MQL," in SAMPE Europe Conference 2021 Baden/Zürich - Switzerland METHOD, Zurich https://doi.org/10.3929/ethz-b-000515235
164. Iskandar Y, Tendolkar A, Attia MH, Hendrick P, Damir A, Diakodimitris C (2014) Flow visualization and characterization for optimized MQL machining of composites. CIRP Ann 63(1):77–80. https://doi.org/10.1016/j.cirp.2014.03.078
165. Park SY, Choi WJ, Choi CH, Choi HS (2018) Effect of drilling parameters on hole quality and delamination of hybrid GLARE laminate. Compos Struct 185:684–698. https://doi.org/10.1016/j.compstruct.2017.11.073
166. Rahman M, Senthil Kumar A, Salam MU (2002) Experimental evaluation on the effect of minimal quantities of lubricant in milling. Int J Mach Tools Manuf 42(5):539–547. https://doi.org/10.1016/S0890-6955(01)00160-2
167. Shyha I, Soo Leung S, Aspinwall DK, Bradley S, Dawson S, Pretorius CJ (2010) Drilling of titanium/CFRP/aluminium stacks. Key Eng Mater 447–448:624–633. https://doi.org/10.4028/www.scientific.net/KEM.447-448.624
168. Kichhannagari S (2004) Effects of extreme low temperature on composite materials. In: University of New Orleans Theses and Dissertations 165. New Orleans, p 105
169. Nagaraj A, Uysal A, Jawahir IS (2020) An investigation of process performance when drilling carbon fiber reinforced polymer (CFRP) composite under dry, cryogenic and MQL environments. Procedia Manuf 43:551–558. https://doi.org/10.1016/j.promfg.2020.02.165
170. Geng D et al (2019) Delamination formation, evaluation and suppression during drilling of composite laminates: a review. Compos Struct 216:168–186. https://doi.org/10.1016/J.COMPSTRUCT.2019.02.099
171. Dilip Jerold B, Pradeep Kumar M (2012) Experimental comparison of carbon-dioxide and liquid nitrogen cryogenic coolants in turning of AISI 1045 steel. Cryogenics (Guildf) 52(10):569–574. https://doi.org/10.1016/j.cryogenics.2012.07.009
172. Pardo A, Heinemann R, Chen CC (2020) The effect of cutting parameter changeover position on interface borehole quality in drilling of aerospace CFRP/Al stacks. Procedia CIRP 101:314–317. https://doi.org/10.1016/j.procir.2020.11.014
173. J Fujiwara, R Nagaura, K Kuroda, and T Tashiro, (2012) "Drilling of CFRP/Ti6Al4V stack board," in ICMT 2012 - 16th International Conference on Mechatronics Technology, Department of Mechanical Engineering, Graduate School of Engineering, Osaka University, Osaka, Japan pp. 285–289.
174. Ismail HN (2016) Sikiru Oluwarotimi, Dhakal E Dimla, and I Popov, "Recent advances in twist drill design for composite machining: a critical review." Proc Inst Mech Eng B J Eng Manuf 231(14):2527–2542. https://doi.org/10.1177/0954405416635034
175. Alphonse M, Raja B, Logesh KVK, Nachippan NM (2017) Evolution and recent trends in friction drilling technique and the application of thermography. IOP Conf Ser Mater Sci Eng 197(1):012058. https://doi.org/10.1088/1757-899X/197/1/012058
176. Alphonse M, Bupesh Raja VK, Gupta M (2019) Optimization of plasma nitrided, liquid nitrided & PVD TiN coated H13–D2 friction drilling tool on AZ31B magnesium alloy. Mater Today Proc 46:9520–9528. https://doi.org/10.1016/j.matpr.2020.03.791
177. R Byakod, HD Gopalakrishna, and S Prasanna, (2014) "Effect of thin film coatings on drill bit," in International Journal of Advance research in Engineering Science and Technology 6–10.
178. Jebaratnam JM, Hassan MH, Mahmud AS, Gérald F (2023) Characterization of nanocomposite tetrahedral amorphous carbon coated drill bits for improved drilled-hole quality in carbon fiber-reinforced polymer/Al7075-T6 stacks. J Compos Mater 57(27):4255–4274. https://doi.org/10.1177/00219983231207988
179. Zhong B, Zou F, An Q, Chen M, Zhang H, Xie C (2022) Experimental study on drilling process of a newly developed CFRP/Al/CFRP co-cured material. J Manuf Process 75:476–484. https://doi.org/10.1016/j.jmapro.2021.12.062
180. Franke V (2011) Drilling of long fiber reinforced thermoplastics - influence of the cutting edge on the machining results. CIRP Ann Manuf Technol 60(1):65–68. https://doi.org/10.1016/j.cirp.2011.03.078
181. Karpat Y, Camuşcu N, Kılıç A, Sonat F, Değer B, Bahtiyar O (2010) Drilling carbon fiber reinforced plastics with diamond coated carbide cutting tools. In: Hinduja S, Li L (eds) Proceedings of the 36th International MATADOR Conference, pp 205–208. https://doi.org/10.1007/978-1-84996-432-6_47
182. Ho-Cheng H, Dharan CKH (1990) Delamination during drilling in composite laminates. J Eng Indust 112(3):236–239. https://doi.org/10.1115/1.2899580
183. Kalidas S, Devor RE, Kapoor SG (2001) Experimental investigation of the effect of drill coatings on hole quality under dry and wet drilling conditions. Surf Coat Technol 148(2):117–128. https://doi.org/10.1016/S0257-8972(01)01349-4
184. Hassan MH, Razali MF (2020) Comparison of coated and uncoated drill bit on the drilling quality of CFRP / AL7075-T6 stacked materials. In: Proceedings of mechanical engineering research day, pp 336–338
185. Laroux Gillespie (2008) Countersinking handbook. Industrial Press Inc.
186. Coromant S (2010) Users guide - machining carbon fibre materials. Sandvik Coromant
187. Sakurai K, Adachi K, Kawai G, Sawai T, Ogawa K (2000) High feed rate drilling of aluminum alloy. Mater Sci Forum - MATER SCI FORUM 331–337:625–630. https://doi.org/10.4028/www.scientific.net/MSF.331-337.625
188. Hamade RF, Ismail F (2005) A case for aggressive drilling of aluminum. J Mater Process Technol 166(1):86–97. https://doi.org/10.1016/j.jmatprotec.2004.07.099
189. Dahnel AN, Ascroft H, Barnes S, Gloger M (2015) Analysis of tool wear and hole quality during ultrasonic assisted drilling (UAD) of carbon fibre composite (CFC) / titanium alloy (Ti6Al4V) stacks. In: Proceedings of the ASME 2015 International Mechanical Engineering Congress and

Exposition, Houston, Texas, USA. https://doi.org/10.1115/IMECE2015-50416
190. Gardiner G (2014) Machining update: one-shot dry drilling of stacked materials. Composites World, Composites World
191. Hassan MH, Abdullah J, Mahmud AS, Supran A (2018) Effect of drill geometry and drilling parameters on the formation of adhesion layer in drilling composite-metal stack- up material. J Mech Eng 5(Specialissue2):90–98
192. Fernández-Pérez J, Cantero JL, Díaz-Álvarez J, Miguelez MH (2019) Hybrid composite-metal stack drilling with different minimum quantity lubrication levels. Materials (Basel)12(3). https://doi.org/10.3390/ma12030448
193. JJoy Mathavan (2023) Investigation of tool coated with tetrahedral amorphous carbon nanocomposite for single-shot drilling of CFRP/aluminium stack. Universiti Sains Malaysia
194. An Q, Chen J, Ming W, Chen M (2021) Machining of SiC ceramic matrix composites: A review. Chin J Aeronaut 34(4):540–567. https://doi.org/10.1016/j.cja.2020.08.001
195. Ramulu M, Wern C, Garbini JL (1993) Effect of fibre direction on surface roughness measurements of machined graphite/epoxy composite. Compos Manuf 4:39–51
196. Arola DD, Ramulu M, Wang DH (1996) Chip formation in orthogonal trimming of graphite/epoxy composite. Compos Part A-appl Sci Manuf 27:121–133
197. Wang DH, Ramulu M, Arola D (1995) Orthogonal cutting mechanisms of graphite/epoxy composite. Part I: unidirectional laminate. Int J Mach Tools Manuf 35(12):1623–1638. https://doi.org/10.1016/0890-6955(95)00014-O
198. J Y Mann and I S Milligan (2013) Aircraft fatigue: design, operational and economic aspects. Elsevier Science.
199. Shanmughasundaram P, Subramanian R (2014) Study of parametric optimization of burr formation in step drilling of eutectic Al–Si alloy–Gr composites. J Market Res 3(2):150–157. https://doi.org/10.1016/j.jmrt.2014.03.008
200. Stringer PG, Byrne G, Ahearne E (2007) Tool design for burr removal in drilling operations
201. Min S, Kim J, Dornfeld DA (2001) Development of a drilling burr control chart for low alloy steel, AISI 4118. J Mater Process Technol 113(1):4–9. https://doi.org/10.1016/S0924-0136(01)00589-1
202. Chen Z et al (2021) Investigation on the Exit Burr Formation in Micro Milling. Micromachines (Basel) 12(8). https://doi.org/10.3390/mi12080952
203. Kundu S, Das S, Saha PP (2014) Optimization of drilling parameters to minimize burr by providing back-up support on aluminium alloy. Procedia Eng 97:230–240. https://doi.org/10.1016/j.proeng.2014.12.246
204. Gillespie LK (1979) Deburring precision miniature parts. Precis Eng 1(4):189–198. https://doi.org/10.1016/0141-6359(79)90099-0
205. Choi I-H, Kim J-D (1998) Electrochemical deburring system using electroplated CBN wheels. Int J Mach Tools Manuf 38(1):29–40. https://doi.org/10.1016/S0890-6955(97)00027-8
206. M Ávila, J Gardner, S Reich-Weiser, Corinne Tripathi, and D Vijayaraghavan, Athulan Dornfeld (2005) "Strategies for burr minimization and cleanability in aerospace and automotive manufacturing," SAE Technical Paper https://doi.org/10.4271/2005-01-3327
207. Sui S, Song G, Sun C, Zhu Z, Guo K, Sun J (2020) Experimental investigation on the performance of novel double cone integrated tool in one-shot drilling of metal stacks. Int J Adv Manuf Technol 109(1):523–534. https://doi.org/10.1007/s00170-020-05474-9
208. Pilny BL (2011) "High speed drilling of aluminium plates," Faculty of Mechanical engineering- Institute of manufacturing technology, p. 151.
209. Dornfeld D (2004) Strategies for preventing and minimizing burr formation. Consort Deburring Edge Finish 19
210. Sreenivasulu R, Rao CS (2019) Overview on Burr formation, simulation and experimental investigation of Burr size — based on Taguchi Design of Experiments during Drilling of Alluminium 7075 Alloy. Int J Technol 7(1):24–30
211. Aurich JC, Dornfeld D, Arrazola PJ, Franke V, Leitz L, Min S (2009) Burrs-Analysis, control and removal. CIRP Ann Manuf Technol 58(2):519–542. https://doi.org/10.1016/j.cirp.2009.09.004
212. Damian B, Daniel K, Piotr M (2017) Deburring and smoothing the edges using vibro-abrasive machining. Procedia Eng 192:28–33. https://doi.org/10.1016/j.proeng.2017.06.005
213. Niknam SA, Zedan Y, Songmene V (2014) "Machining burrs formation & deburring of aluminium alloys," W. A. Monteiro, Ed., Rijeka: IntechOpen, p. Ch. 5. https://doi.org/10.5772/58361
214. Davim J, Campos Rubio J, Abrao A (2007) A novel approach based on digital image analysis to evaluate the delamination factor after drilling composite laminates. Compos Sci Technol – COMPOS SCI TECHNOL 67 1939–1945 https://doi.org/10.1016/j.compscitech.2006.10.009
215. Haeger A et al (2016) Non-destructive detection of drilling-induced delamination in CFRP and its effect on mechanical properties. Procedia Eng 149(June):130–142. https://doi.org/10.1016/j.proeng.2016.06.647
216. Gaugel S et al (2016) A comparative study on tool wear and laminate damage in drilling of carbon-fiber reinforced polymers (CFRP). Compos Struct 155:173–183. https://doi.org/10.1016/j.compstruct.2016.08.004
217. Yuan Jia Z, Zhang C, Ji Wang F, Fu R, Chen C (2020) Multi-margin drill structure for improving hole quality and dimensional consistency in drilling Ti/CFRP stacks. J Mater Process Technol 276:116405. https://doi.org/10.1016/j.jmatprotec.2019.116405
218. Silva DNR Da (2013) Image processing methodology for assessment of drilling induced damage in CFRP. Universidade Nova de Lisboa
219. Mehta AH, Reinhart M, Soni TJ (1992) Effect of fastener hole drilling anomalies on structural integrity of PMR-15/Gr composite laminates. In: ASM; Materials Shaping Technology Division; Machining Committee TMS; Machining of composite materials, pp 113–126
220. Tsao CC, Kuo K, Hsu IC (2012) Evaluation of a novel approach to a delamination factor after drilling composite laminates using a core–saw drill. Int J Adv Manuf Technol 59:617–622
221. Xu J, Li C, Mi S, An Q, Chen M (2018) Study of drilling-induced defects for CFRP composites using new criteria. Compos Struct 201. https://doi.org/10.1016/j.compstruct.2018.06.051